DEVELOPMENT OF A SUBSURFACE WATER VELOCITY AND QUALITY MEASUREMENT PAYLOAD FOR SUAS

by

Mitchell Bailey

A thesis submitted in partial fulfillment
of the requirements for the degree

of

MASTER OF SCIENCE

in

Electrical Engineering

Approved:

Sierra Young, Ph.D. Major Professor	Calvin Coopmans, Ph.D. Major Professor
Burak Sarsilmaz, Ph.D. Committee Member	D. Richard Cutler, Ph.D. Vice Provost of Graduate Studies

UTAH STATE UNIVERSITY
Logan, Utah

2024

ABSTRACT

Development of a Subsurface Water Velocity and Quality Measurement Payload for sUAS

by

Mitchell Bailey, Master of Science

Utah State University, 2024

Major Professors: Sierra Young, Ph.D. , and Calvin Coopmans, Ph.D.
Department: Electrical and Computer Engineering

The growth in aquaculture has not been followed by an equal increase in water monitoring techniques. The methods used to monitor aquaculture farms often involve stationary in-situ sensors used after specific weather events. This reactive or stationary measurement results in temporal and spatial gaps in data containing event bias, so data is not representative of nominal water conditions. An Uncrewed Aerial System (UAS) payload capable of rapid data collection has been developed in this thesis to solve these issues. Current UAS remote sensing methods cannot measure velocity or other important parameters beneath the water's surface, so submerged sensors are used. The payload utilizes a tethered probe to collect depth-velocity profiles in shallow ($< 2m$) water in under 2 minutes. The probe can break away from the UAS through a magnetic release to ensure UAS safety. Tests in controlled water flumes reverse-engineered the sensor's communication protocol and applied it to the payload. The sensor was used in irrigation canals with less than 3% mean error compared to the traditional datalogger, validating the payload's ability to operate as an alternative datalogger. When deployed from a bridge over a channel, the sensor measured with less than 2% mean error compared to a nearby Acoustic Doppler Channel Profiler (ADCP). Deployment on a UAS in a coastal channel with natural oyster leases showed the

payload's much faster deployment times than current water velocity measurement methods, with payload deployment taking under 15 minutes. The payload was able to measure depth-velocity profiles with success, dependent on the orientation of the probe. With proper alignment, the UAS deployed payload had mean error as low as 3.89% compared to measurements from a nearby ADCP. With proper orientation the payload can operate as a rapidly deployable velocity sensor able to provide better resolution to aquaculture data sets and inform the need for more precise sensing. Both probe orientation and low sample count at specific depths contributed to the sensor's error, with sample count addressed through longer measurement times and precise depth control. Additional work on active probe orientation control methods would solve the most significant source of error.

(68 pages)

PUBLIC ABSTRACT

Development of a Subsurface Water Velocity and Quality Measurement Payload for sUAS

Mitchell Bailey

Aquaculture farms, like oyster farms, often use outdated techniques to measure the quality of their waters. These techniques are often stationary or are deployed by an operator who may struggle to reach a location depending on conditions like the presence of a storm or low tide. This creates data sets with gaps over time and across the area of the farm, meaning the data cannot be used to model the standard farm conditions. An Uncrewed Aerial System (UAS) payload is developed in this paper that is capable of measuring depth-velocity profiles through the use of a tethered velocity sensor. The tether is able to detach from the UAS through a magnetic release to ensure UAS safety. Controlled water flumes helped in the reverse-engineering of the sensor's communication protocol. Tests in irrigation canals demonstrate the payload's ability to measure in place of the traditional datalogger with less than 3% mean error. The payload was able to successfully measure the velocity of a coastal water channel when deployed from a bridge with less than 2% mean error. The payload was able to be deployed on a UAS in under 15 minutes by one person, which is much faster than other water velocity measurement methods. The payload was able to measure around 10 locations per flight and was moderately successful at measuring the depth-velocity profile of the locations. When the sensor was properly aligned in the direction of the water flow, the sensor had mean errors as low as 4%. However, misalignment and low sample count caused other locations to have errors as high as 31%. Low sample count is easily solved through the use of better depth control and longer sampling times. Future work needs to be done on sensor orientation control to limit that source of error.

ACKNOWLEDGMENTS

I want to thank both Dr. Sierra Young and Dr. Calvin Coopmans for providing me with the opportunity to work on a project as interesting as this one. The support and guidance provided by both of my advisors are why this project was able to succeed. This project allowed me to learn both electrical engineering and environmental sensing and has shaped my future career path into one of research.

I would also like to thank the North Carolina team for their hard work during the field campaign of this project.

Thank you to my parents, whose encouragement and support are why I was able to make it this far. A special thank you to my friends, who traveled over a thousand miles to visit me.

Mitchell L. Bailey

CONTENTS

LIST OF TABLES

LIST OF FIGURES

ACRONYMS

ADCP	Acoustic Doppler Current Profiler
EMV	Electro-Magnetic Velocity
LDV	Laser Doppler Velocimetry
MSV	Manual Surface Vehicle
PIV	Particle Image Velocimetry
sUAS	Small Uncrewed Aerial System
UAS	Uncrewed Aerial System
USV	Uncrewed Surface Vehicle
UWRL	Utah Water Research Laboratory

CHAPTER 1

INTRODUCTION

Aquaculture is the fastest-growing protein sector within the agriculture industry, but the methods used to monitor its farms have not equally progressed [1]. Current water monitoring methods in aquaculture consist of in-situ sensing and sample collection by operators in or near the farm's waters. These processes are expensive and result in minimal data collection, often only after notable events such as storms. This practice creates data sets with data biased towards these events, making them unusable for modeling or analysis of the environment. Alternatively, a sensor is installed on a farm for months at a time, resulting in biofouling and corrosion on the sensor. These lower the sensors' performance and eventually stop them from measuring, requiring expensive maintenance and replacements [2].

There are several reasons why measuring water velocity is important for aquaculture. With known channel dimensions, point water velocity measurements can be used to estimate the volumetric discharge of a channel. Measuring velocity is often done with Acoustic Doppler Current Profilers (ADPC), which are expensive and slow to deploy into the water, resulting in infrequent use and poor data sets. Another method is Particle Image Velocimetry (PIV), typically captured by Uncrewed Aerial Systems (UAS). This method is much faster and cheaper to deploy than an ADCP and can capture velocity with much better spatial resolution completely remotely from the water. However, PIV is only able to measure the surface velocities of water, and channel models must be used to estimate the subsurface velocities. The method also loses accuracy without the use of particle seeding, where easily visible material is introduced into the flow [3]. Particle seeding increases the complexity of measurement, increasing cost and slowing down the process.

1.1 Problem Statement

The field of aquaculture currently relies primarily on in-situ measurements for water

quality monitoring. Unoccupied Surface Vehicles (USV) or manual Surface Vehicles (MSV) are both limited by conditions such as weather, tide, and budget. This can lead to a decline in the frequency of monitoring, creating data sets without enough temporal or spatial resolution to capture water quality dynamics and make effective decisions regarding harvest closures or openings. Without proper data sets, predictions regarding the condition of the water are biased towards storms and rain. This becomes especially problematic in oyster farms, where fecal coliform in water runoff can contaminate the oysters with bacteria, making them unsafe to eat. The fecal coliform content in the water can be related to the velocity and salinity of the water, which are not quickly measured by current methods. By quickly monitoring these qualities in farms, food safety is improved, and better data sets are created.

An Unoccupied Aerial System (UAS) is able to take quick measurements during conditions such as rough or low waters at a faster and cheaper rate. Current techniques exist to allow UAS to measure the velocity and temperature of water streams at the surface level. However, these techniques fail to capture subsurface measurements, which are important for aquaculture monitoring or channel characterization.

1.2 Project Goals

To improve the rate of data collection in aquaculture, the payload was designed to be deployed faster than current methods for collecting depth-velocity profiles. The payload is able to collect these profiles in under two minutes per location, with little time spent transitioning between locations because of the UAS's speed. The payload was designed with low-weight sensors suitable for UAS deployment, which were validated in several lab tests. Because of the nonrigid cable used to tether the sensors, probe orientation relative to the UAS cannot be guaranteed. Therefore, a flight method capable of correcting for this was used and tested in several flights. The floor of water bodies can contain unknown debris that is not visible to the pilot, presenting a potential hazard for the probe to be stuck on. This is why a magnetic release mechanism between the tether and the UAS was created to allow for detachment.

1.3 Objectives

The objectives of the payload are the following:

1. Measure the velocity-depth profile of a location in a water body faster than current methods.

2. Compensate for lateral UAS drift or misalignment of probe orientation relative to water flow direction.

3. Detach the tether and probe from the UAS should the probe be caught in debris in the water.

Increasing the speed of velocity measurement reduces costs for farms and increases the resolution of data sets. Fast measurement is also important for maximizing UAS battery usage, increasing the amount of points measured. The sensors were first reverse-engineered and verified in controlled waters and then moved to field testing environments. Testing the effect of probe orientation in moving water created a relation between the probe orientation and measurement value. This is necessary for post-processing and ensuring the measurements are accurate. The detachment method consists of magnetic connections that passively break only under excessive force achievable by the UAS. Finally, the payload was flown in a coastal tidal channel and used for depth velocity profiling alongside traditional measurement methods.

CHAPTER 2

Background

2.1 Water Sensing Methods

The quality of the waters of aquaculture farms is essential to monitor as they can determine the safety of the food being grown. Water velocity can be measured to monitor rain runoff, which correlates to incoming freshwater or farm runoff. Velocity is commonly measured with in-situ sensors, ADCPs, and Imaging techniques, which measure points, one-dimensional profiles, and two-dimensional maps, respectively. Other water qualities like salinity or dissolved oxygen are needed at specific levels for specific foods. These qualities can be measured with in-situ sensors or by collecting water samples.

2.1.1 In-Situ Methods

In-situ sensors are placed directly into the water at the point of measurement rather than remotely measuring from a distance. They can be momentarily placed to record a measurement or installed and left for a more extended period of time. A prominent method of water quality measurement in aquaculture is using long-term in-situ sensors that remain in a single location for months at a time. Exposure to the environment for so long causes sensor degradation from effects such as biofouling, eventually preventing sensor operation. Efforts to minimize the impact of biofouling on these sensors have been studied to lower the operational costs needed in maintenance [2]. Although not commonly discussed, aquaculture can negatively impact the surrounding environment through organic waste and the release of toxic chemicals [4]. The use of in-situ sensors in aquaculture farms allows for the monitoring of these impacts, which can be used to inform better farming decisions [5]. However, these sensors often capture only a single point in a farm, resulting in poor spatial resolution in data sets.

One prominent type of in-situ velocity sensor is the Electro-Magnetic Velocity (EMV) meter. They are sensors that produce a magnetic field into the water and measure the rate at which water passes through it. They are often handheld and held stationary beneath the surface of the water. The use of EMV meters has grown in recent years because of the ability to operate in sediment-choked waters and low flows, two areas where ADCP performance is impeded [6]. EMVs have a low environmental impact and are robust to the less ideal conditions of coastal environments, which have more turbulence. Another form of velocity measurement used is Laser Doppler Velocimetry (LDV), which records particle velocity in water as an alternative to ADCPs. LDV is used in deeper conditions but performs worse than ADCPs at low velocities (< 1 m/s), making them unfavorable for coastal measuring [7].

In-situ measurements are usually taken by an operator in the water or on a boat when taking measurements, both of which take long periods to deploy. Remote hydrology measurement reduces the cost and time of sending operators to sites and often speeds up monitoring. It has become more common for in-situ sensor packages to be equipped with means for remote data transfer, allowing operators to monitor site conditions remotely [8]. To additionally reduce the cost of ground operators handheld sensor packages are becoming more simplified for use by less trained operators. An inexpensive multi-sensor package was designed with a smartphone application as the monitoring method [9]. This further demonstrates the current importance of cost reduction in hydrology in the form of reducing operator and equipment costs.

2.1.2 Acoustic Doppler Channel Profiling

The Acoustic Doppler Channel Profiler measures the Doppler effect on acoustic noise from moving water to determine the water's velocity along a single direction. ADCPs are widely used because of their reliability over a wide range of conditions, including stream widths, depths, and velocities. They have been widely tested against existing velocity measurement methods with comparable results that validate their use as a velocity measurement tool in hydrology [10]. They do not have much environmental impact as they barely disturb

the waters they are in. When an ADCP is used, it can gather the velocities of points in a straight line in the water, giving a one-dimensional velocity profile that can be combined with known water channel models to estimate the velocity at other points of the channel.

ADCPs are used to measure the discharge of tidal channels because they can estimate the subsurface flow based on surface velocities and known channel geometry. However, significant error can occur due to cross-sectional differences in salinity and temperature [11]. ADCPs are often placed on river banks to measure the surface velocities across a cross-section of a channel. However, it is possible for ADCP use on floating, mobile platforms on the water's surface. Tidal elevation was also measured using a towed boat ADCP, which found both tidal velocity and elevation of a water channel [12]. It is important that the water conditions are calm enough that the ADCP doesn't experience excess motion. A horizontal ADCP was used in a boat to collect surface water velocities but contained inaccuracies due to the movement in the boat in rough waters [13]. Other watercraft, such as those towing the ADCP, can cause large wakes in water, and ADCP data requires more post-processing when operating around them. The data from mobile ADCPs can be used to estimate velocity profiles despite turbulence caused by the presence of towing boats through special processing [14].

ADCPs can also be anchored to nearby structures rather than being towed, allowing use near tidal energy platforms. While on these floats, ADCPs successfully determined the new velocity profiles of the volume of water surrounding the platform [15]. One downside of ADCP measurements is that they are impacted by the presence of particles in the water that cause the acoustic signal to backscatter before reaching the floor of the water channel. However, ADCPs can use this effect to measure the particle size and particle concentration in the waters, allowing for back calibration [16].

2.1.3 Particle Image Velocimetry

Imaging in hydrology is a common technique for surface velocity measurement of an area. PIV is a measurement technique that tracks individual particles between image frames to determine their speed. The advantage of PIV is the simultaneous recording of entire areas,

with spatial resolution tied to camera resolution, which allows for much better resolutions than in-situ sensors. This means PIV can be used to track wide areas of shallow flow and identify the present flow structures with relatively basic equipment [17]. Additionally PIV requires significantly less calibration compared to other methods like ADCP, allowing them to be deployed much faster.

Airplane-flown cameras have been used to characterize tidal flows alongside riverbank stationary Doppler radars, which found channel cross-sections [18]. These techniques were able to measure surface velocity and model the subsurface velocity profile but did not directly observe subsurface velocities. Additionally, airplanes are not a sustainable nor rapidly deployable form of remote sensing, which is further slowed down by the need for ADCP installation at the same site.

One benefit of PIV as a method is that it prevents contact with the water, which can disturb both the environment and the water's flow. PIV sometimes involves particle seeding to create prominent and known particles for the algorithm to track. A comparison of PIV with and without seeding was conducted, and it found that without seeding, PIV will have greater mean absolute error [19]. Seeding is problematic for rapidly deployable sensing because it adds complexity to the technique and requires more time before measurements can be taken. Additionally, it adds material to the water, meaning the method is no longer completely removed from the water body.

PIV is not a new technology and has been used in environmental monitoring and laboratory fluid flow measurement. PIV is a tested enough technique that it is relied on now to confirm the behavior of simulations. PIV was used on a water-air mixing tank to validate and refine the existing theoretical behavior of the complex, turbulent flow [20]. PIV can also be used to evaluate properties of water flow other than water velocity. Water turbulence in the surface of river discharge can be measured using PIV with similar results to an ADCP [21].

PIV is an excellent remote technique with less expensive equipment than other currently used velocity measuring techniques. Because PIV relies on a camera, it is easily deployed

by UAS, which are commonly used for picture and video in a variety of industries. This allows for faster deployment and a better, more adjustable field-of-view, which is important for imaging.

2.2 UAS-Based Methods

In-situ measurements cannot respond to a sudden change in environment, such as a flood, as they take time to install, and their operators cannot approach the flood safely. Satellite measurements are fixed in their distance, resulting in datasets with much worse spatial resolution than what might be needed to assess specific locations. UAS usage in hydrology bridges the gap between traditional ground-based and satellite measurements through a wider range of spatial and temporal resolutions. The UAS as a platform is faster than ground operators and can access locations regardless of many factors, such as hazards or available ground paths. These advantages are why UAS have become standard tools used in many forms of hydrological research [22]. They have already been documented as more cost-effective than satellite and in-situ sensing thanks to improvements to their technology [23].

2.2.1 Drone-Based PIV

Because of the rise of UAS-based PIV, UAS have been specifically designed for use in PIV, with a focus on low-cost, stable platforms [24]. Because waterproofing UAS components is difficult and expensive, low-cost UAS can instead be replaced in the event of a crash. This lowers the entry barrier for using UAS in hydrology by smaller farms or research labs. However, UAS as a platform is susceptible to both wind and compass drift, resulting in non-stationary imagery, which is detrimental to interpolating between frames in PIV. Corrections have been found to rectify images that have suffered from UAS drift to increase the accuracy of PIV measurements [25].

There exist several algorithms for PIV that are commonly used with UAS imagery: Large Scale Particle Image Velocimetry, Large Scale Particle Tracking Imagery, Kanade-Lucas Tomasi Image Velocimetry, Optical Tracking Velocimetry, and Surface Structure

Image Velocimetry [3]. These techniques have all been verified to measure water surface velocities with little difference in results compared to ADCP measurements. However, these comparisons rely on seeding the water with more visible particles, adding to the complexity of remotely sensing water bodies.

In addition to RGB imagery, thermal imagery can also be used in UAS-based PIV with similar results. Thermal infrared cameras are a new technology used to record water velocities as well as water temperature through PIV techniques. The water surface velocity of a river was measured with both RGB and thermal infrared cameras and saw similar results between both datasets [26]. The use of UAS in hydrology has helped identify processes that drive streamflow in headwaters because it is able to achieve higher resolutions with thermal infrared cameras than ground operators [27].

UAS-based PIV is beginning to replace ADCP measurements because it is fundamentally cheaper, non-invasive, and faster to deploy than ADCP. ADCP typically rely on models to make estimations of channel cross-sectional behavior. PIV can be used to validate existing hydraulic models similarly to ADCP measurements with comparable results [28].

In-situ measurements of tidal measurements are currently expensive and have a spatial-temporal separation of the measured points, creating incomplete datasets. UAS-based PIV offers a potentially cheaper alternative for tidal steam measurement to traditional ADCP measurements. Using large-scale PIV, it is possible to achieve better spatial coverage and accurate first-order tidal measurements with UAS with significantly faster deployment times [29]. Additional work has shown that PIV can operate in a wide range of wind speeds despite the presence of wind ripples on the surface of the water with accuracies of 5-6% for high wind scenarios [30].

One example of an environment that is difficult to measure by ground operators is mountain rivers, which UAS are able to reach easily. New techniques for measuring mountain river velocities using UAS space-time image velocimetry have proven that the UAS can reliably measure these without the need for ground operators [31].

Another environment suited for UAS-based PIV monitoring is ephemeral streams that

only contain water occasionally. Ephemeral streams require measurement during very specific times, meaning that measurement must be rapid. They can also be difficult to reach by grounded operators depending on their location. This is why UAS have been deployed with PIV to successfully map the surface velocities of ephemeral streams and low discharges [32].

Because PIV is based on imaging, it cannot measure subsurface velocities and is limited by line-of-sight. Because particle tracking assumes the same particles will be in every frame, the existence of objects in the field of view that obscure the water can cause PIV to become less accurate. Three different PIV software were tested in UAS flights over rivers, and all suffered significant differences in velocity due to the presence of vegetation along the river [33].

2.2.2 Drone-Based Quality Sensing

UAS are becoming more common in environmental research but are used for remote imaging far from the data they collect. Close proximity UAS flights that involve direct sensing allow for different measurement methods that can capture additional qualities, such as water sample collecting or direct conductivity measurements, which are impossible with remote sensing. UAS do not require shoreline access and deploy faster than water surface vehicles, making them useful for in-situ sensing, which requires either operators or vehicles. Not only are operator-gathered in-situ measurements more expensive and slower than UAS-gathered ones, but they also are less representative of the distributions in the water body because of the disturbance caused by the operator [34].

Use of open-source components for hydrology is another potential way to reduce cost and allow for use in custom payloads, such as UAS payloads. Measurements of water temperature, dissolved oxygen, conductivity, and acidity were conducted through the use of a UAS with both open-source and commercially available measurement packages showing little difference in measurements [35]. This is important for small farms or research labs as the cost of commercially available sensor packages is much higher than open-source packages.

Temperature is commonly recorded with thermal infrared cameras, which are only able to record surface temperature. However, it can be valuable to detect subsurface tempera-

tures. Temperature measurements below the surface of a lake were taken with a tethered temperature probe attached to a UAS [36]. A small probe being the only contact with the water improves the representation of the measurement, which an operator would otherwise disrupt.

In-situ sensors also present an opportunity to be used as an observer for UAS controls. Tethered pressure transducers have been used from UAS to record the current depth of a probe, which was fed into a control loop to precisely control the UAS's altitude [37]. This allows for more advanced flight techniques near water and can benefit other UAS in-situ measurements by ensuring better target depth holding.

Water sample collection is used to identify or measure contaminants in the water that are not easily detected in the field. Samples are commonly collected by operators in the water but have begun to be collected by UAS payloads. Water sample collection by UAS minimizes the amount of interaction with the water body that would otherwise be disturbed by the operator or boat used in collection. A payload both collecting water samples and measuring in-situ water qualities has been developed for use in difficult-to-access water bodies [38]. Water sample collection by UAS has been validated as an alternative approach that is comparable to existing approaches [39].

The benefit of using UAS in hydrology is the autonomous nature of the systems. Autopilot software is commonplace, and autonomous measuring or sample collection can reduce the time spent at a site, which is critical for UAS with limited flight times. Researchers have already created payloads capable of autonomous in-situ water measurement and water sample collection [40].

UAS water sample collection has been used successfully to detect the presence of DNA in water bodies because the UAS offers improved spatial and temporal resolution when compared to the current sample collecting methods [41]. This allows for the same results as operator sample collection with much shorter sampling times.

Breakaway connectors have been used to detach tethered payloads from UAS because of the risk tethers pose to the UAS. A UAS payload consisting of a subsurface water tem-

perature probe was designed with a magnetic breakaway mechanism to measure power plant water plumes [42]. Reducing the risk of total UAS failure over water reduces the cost of operation of in-situ sensors from UAS.

Current velocity sensing methods are in-situ, which are expensive in time and cost of labor, or remote, such as PIV, which are rapidly deployed by UAS but fail to measure subsurface qualities. By combining the deployment method of a UAS with the sensors used in in-situ sensing, rapidly available velocity sensing can be achieved. This can be used to improve the quality of aquaculture farms by deploying quickly after events, informing the use of additional sensors, and supplementing datasets through better spatial and temporal resolutions.

CHAPTER 3

Design and Methodology

The payload was designed to lower a set of sensors into the water from a cable underneath the UAS in order to get subsurface measurements. Velocity and pressure sensors were chosen to be lightweight, small in size, and fast in measurement to optimize the payload for use by a UAS. Magnetic releases are employed to ensure the safety of the UAS. The velocity sensor used was reverse-engineered to circumvent the manufacturer's datalogger.

3.1 System Overview

The purpose of the payload is to measure water velocity by lowering a sensor into the water from a UAS. The payload is a combination of a Raspberry Pi acting as a datalogger, a set of sensors on a submerged probe, a cable with magnetic release, and a downward-facing camera. As shown in Figure 3.1, the probe is made of a velocity sensor, pressure sensor, and conductivity sensor with a carbon fiber spar between the velocity sensor and the other sensors. The reason for the spar is to have the other sensors act as a weight on a lever arm, keeping the velocity sensor's pitch level. The datalogger is a Raspberry Pi with buck converters to provide power from the UAS, an RS485 adapter to communicate with the velocity sensor, and magnetic connectors for sensor communication shown in Figure 3.2. The payload is modular and able to use additional sensors if needed, such as a dissolved oxygen sensor. To allow for cable disconnection, a magnetic release system supports the weight of the cable and probe with permanent magnets shown in Figure 3.3

3.2 Velocity Sensor

The payload was designed for a coastal environment with the potential for debris-filled and turbulent water. The maximum velocities expected in these environments are under 1 m/s, so sensors need to be designed for these lower velocities. Because the payload is

Total Mass	1.114 kg
Cable and Probe Mass	0.9 kg
Datalogger Mass	0.214 kg
Power Consumption	4.8 W
Sampling Rate	$\tilde{5}$ Hz

Table 3.1: Summary of Payload Specifications

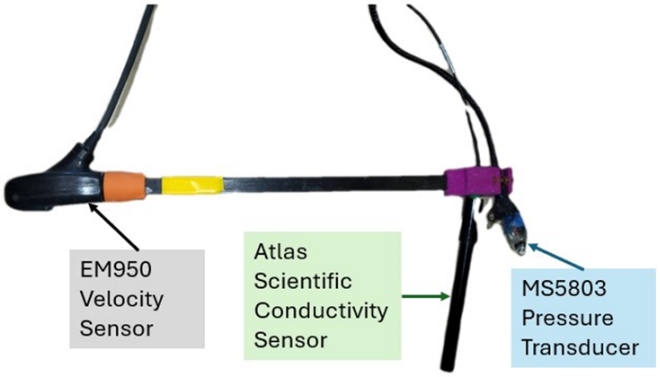

Fig. 3.1: A Picture of the Payload's Probe.

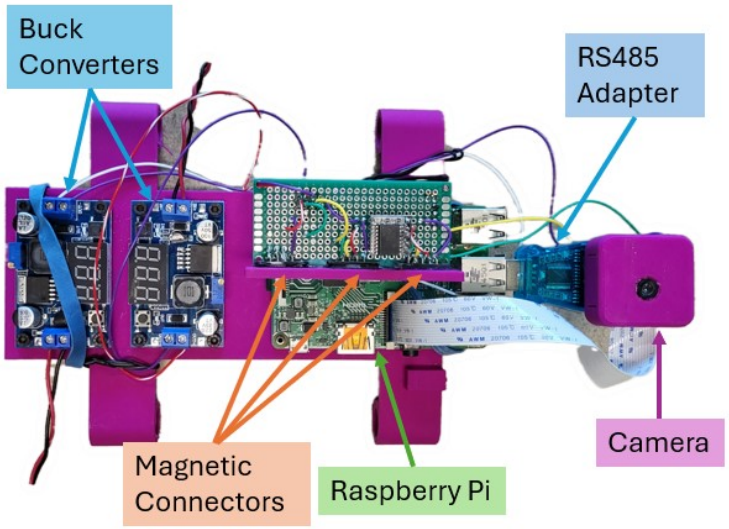

Fig. 3.2: A Picture of the Payload without the Probe or Cable.

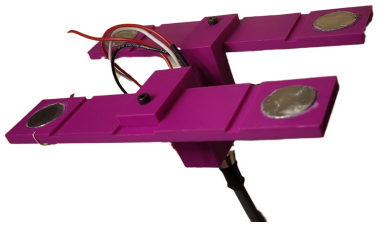

Fig. 3.3: A Picture of Magnetic Support Mount with Cable Attached.

UAS deployed, the sensors should be under 1 kg to maximize flight time. Several different sensors were considered for use on the payload, including several popular sensors within hydrology. Many in-situ velocity sensors currently used in hydrology were too heavy or were not designed for low velocities. The velocity sensor used in this payload is the EM950 Velocity Sensor (Hach, Loveland, CA), which is an industry-standard sensor for shallow (less than 5 feet depth) measurement of rivers and channels.

3.2.1 Sensor Description

The EM950 is a small sensor designed for handheld use by a single operator in shallow water, typically in environments like rivers or urban drainage systems. It is designed for use with an adjustable rod that acts as a depth gauge to hold at a specific, constant depth. It models stream flow by either recording single-point measurements and estimating channel geometry or by measuring entire cross-sections by measuring multiple points of the channel. The sensor is used with a proprietary datalogger to record and store measurements and cannot be used with alternative dataloggers by default, such as autonomous systems. To remedy this, the datalogger's communication protocol was decoded and replicated by the Raspberry Pi for use on a UAS payload. When used in this payload, the sensor freely hangs from its cable, which offers minimal control of the sensor's orientation in the water.

3.2.2 Sensor Operation

The sensor measures the magnetic field in passing water to measure the speed of water in the direction the sensor is orientated. Because of this, the sensor can work in turbulent and murky water but must be orientated in the direction of flow. One end of the sensor

Sampling Rate	6 Hz
Accuracy	+/- 0.015 m/s
Velocity Range	0 to 6.1 m/s
Temperature Range	-20 to 55 °C
Dimensions	11.9 $\times$4.3 $\times$ 6.3cm
Communication	RS485, UART

Table 3.2: EM 950 Velocity Sensor Specifications

Fig. 3.4: A Picture of the Hach EM950 Velocity Sensor.

has a bracket that allows it to be mounted to an adjustable depth holding rod to maintain a constant depth.

Because the velocity sensor must be oriented into the water flow, the spar acts as a counterweight to level the sensor's pitch. The lateral orientation of the sensor is not guaranteed in the water as the sensor cable is not rigid. Because of this, the aircraft must yaw to correct the sensor orientation. This only provides minimal control over the probe's orientation, especially when the probe is submerged so it is still possible for the sensor not to be directed in the direction of flow. To account for this misalignment when operating, the sensor is rotated via the aircraft to measure a large range of angles relative to the direction of flow so that the highest record velocity is the in-line velocity.

3.2.3 Reverse Engineering of the Sensor Signals

The EM950 is designed for use with a proprietary datalogger, which does not have open-source software. The communication between the datalogger and sensor was decoded and recreated to use a Raspberry Pi as an alternate datalogger. To begin recording the sensor's communication, the sensor, Hach datalogger, and Raspberry Pi were wired together

Sampling Rate	60 Hz
Accuracy	+/- 2.5 mBar
Pressure Range	10 to 1300 mBar
Temperature Range	-40 to 125 °C

Table 3.3: MS5803B Pressure Transducer Specifications

so that the Raspberry Pi could intercept the command from the datalogger, record it, and then send it back to the sensor as depicted in Figure 3.5. The sensor would then send a response to the command to the Raspberry Pi, which would be recorded and sent to the datalogger. This process was repeated until the datalogger and sensor would repeat a single command and response respectively. This response from the sensor contained the measurements it had gathered at the time of the command.

The measurements can be verified through a diagnostic screen on the datalogger, shown in Figure 3.6. This screen contains both ‘raw‘ hexadecimal values for velocity and their corresponding measurements in m/s. The ‘raw‘ values are directly from the sensor and have not been converted. By recording the screen, each ‘raw‘ value and its corresponding value in m/s are paired which allows for conversion by the Raspberry Pi.

3.3 Pressure Sensor

To obtain a velocity depth profile, information is needed regarding the depth at which each velocity sensor measurement is obtained. Because the exact depth cannot be guaranteed by UAS altitude alone, a pressure sensor is used to record water pressure, which is converted to depth. The pressure sensor used is the MS5803B (TE, Schaffhausen, Switzerland) pressure transducer, which is a common, off-the-shelf pressure sensor that communicates through I2C communication and can collect both pressure and temperature data. Temperature measurement allows for temperature correction of pressure measurements, increasing the sensor's accuracy and allowing for temperature profile measurement of the water.

3.4 Magnetic Release

The sensor cable is 6 m long which presents a potential hazard for the UAS in the

Fig. 3.5: Capture and Recording of the Datalogger Commands uses Four Steps to Record and Mimic Sensor Communication.

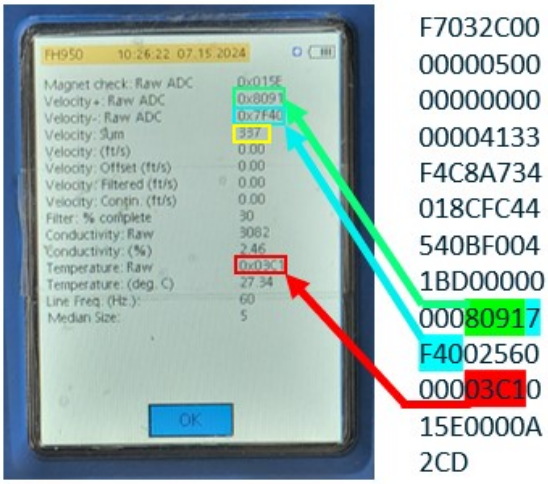

Fig. 3.6: Hach Datalogger Diagnostic Screen and Bytes from Data String from Sensor can be Matched to Identify Useful Values.

Fig. 3.7: Picture of the MS5803 Pressure Transducer Used to Record Probe Depth.

event it becomes caught on trees or underwater debris. A magnetic release was designed to allow the cable to separate under high enough forces. There are two sets of magnetic connections: one for supporting the weight of the cable and probe and one for connecting the wires of the payload to the sensor. The supporting magnets, shown in Figure 3.3, release at a force of approximately 29 N (3 kg), which was designed to be easily achieved by a UAS. The connection magnets on the Raspberry Pi release under very small forces and are not intended to support any weight but to maintain sensor communication. Both sets of magnets were aligned with 3D-printed mounts to prevent shearing apart.

3.5 Datalogger and Wiring

The datalogger used was a Raspberry Pi because of its flexibility and ease of use. As shown in Figure 3.8, the pressure and conductivity sensors and an external real-time clock were connected through SDA and SCL pins for I2C connection. The velocity sensor required an RS485 adapter, which was connected through a USB port. The entire payload

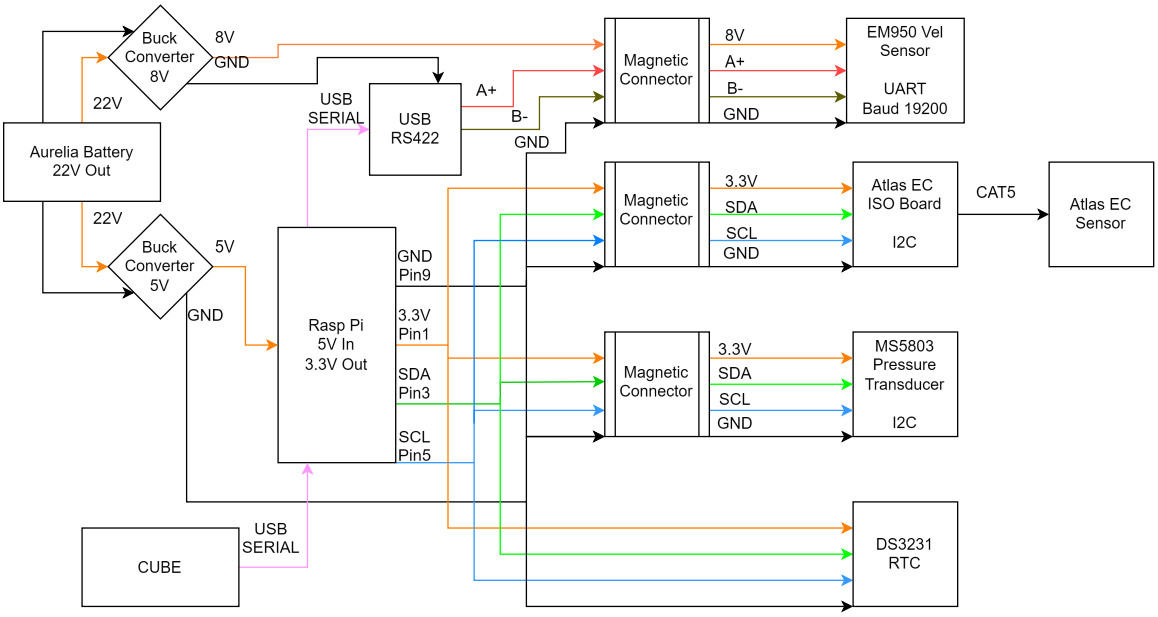

Fig. 3.8: The Wiring Diagram of the Payload's Power and Communication

used power from the UAS 24 V battery, which was connected to buck converters to produce 8 V power for the velocity sensor and 5 V power for the Raspberry Pi and pressure sensor.

3.6 Velocity Sensor Calibration

Because the velocity sensor is not using the manufacturer's datalogger, the conversion from the sensor's hexadecimal measurement into a usable unit must be verified.

3.6.1 Velocity Magnitude Calibration

First, the magnitude of the sensor reading while properly oriented is measured with both the Raspberry Pi and the manufacturer datalogger. Tests were conducted in a controlled water flume in the Utah Water Research Laboratory (UWRL) with flume dimensions of about 61 cm height and 76 cm width and water height at roughly 30 cm. The flume was set to a water velocity of 15 cm/s at 13 cm depth and was held constant for the remainder of the test. The probe was held in place at a consistent 13 cm depth facing into the flow for 30 seconds, as shown in Figure 3.9, collecting measurements every 0.2 seconds. Then, the probe was removed and the Raspberry Pi was replaced with the manufacturer's datalogger,

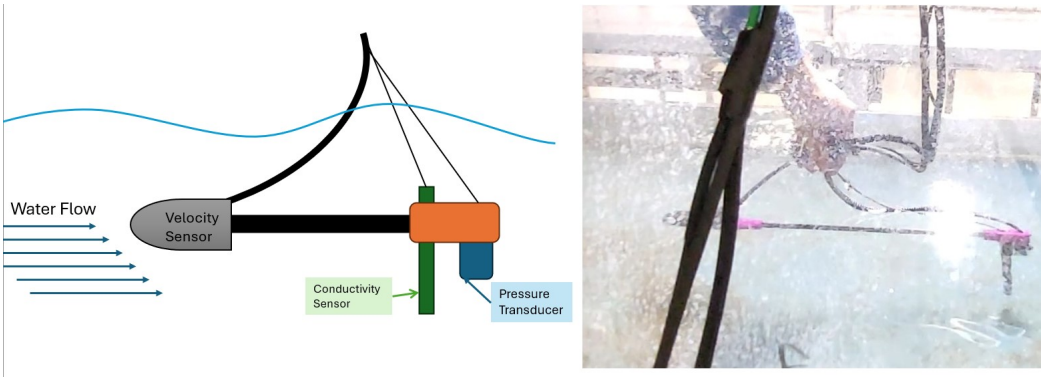

Fig. 3.9: The Calibration Tests that Verified the Payload's Communication with the Sensor were Performed in a Water Flume shown in the Diagram and Image.

which acted as a ground truth velocity measurement. After each test, the water velocity was increased by 10 cm/s and the test was repeated. The arbitrary hexadecimal and ground truth m/s values were recorded every half second. The sensor produced identical values with both the Raspberry Pi and the manufacturer datalogger for a given velocity, meaning only the relation between arbitrary hexadecimal and m/s values needed to be found.

A second-order polynomial model was fit to the data to find the conversion method shown by the orange line in Figure 3.10. The resulting model was $v(x) = 1.272 * 10^{-7}x^2 + 0.00175x$. Higher-order models were fitted but had similarly negligible coefficients for higher-order terms, showing only the linear term is significant. When testing in still water, the sensor produces a reading of 0 for 0 m/s, which is why there is no constant offset for the calibration curve. The p-value associated with all coefficients was less than 0.001. Therefore, the conversion from the sensor's arbitrary reading to m/s was found to be a multiplication of 0.00175 by the hexadecimal value from the sensor. The results of testing are shown in Figure 3.10 in blue, with the curve fit shown in orange. The calibration was done with three different tests shown by the groups in Figure 3.10.

3.6.2 Velocity Measurement at Varying Angles

In another set of tests at the UWRL, the probe was rotated to determine the velocity sensor's response to being misaligned with the primary direction of the flow of water. Water

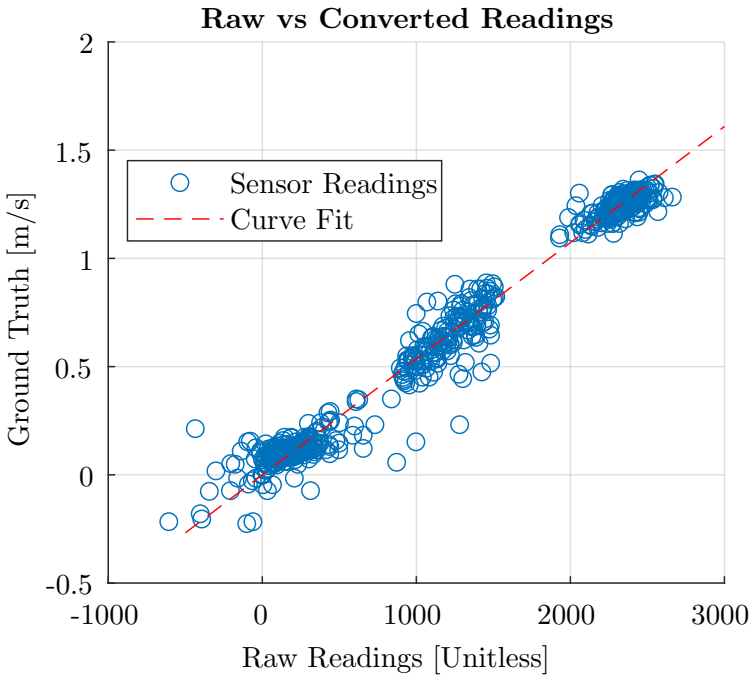

Fig. 3.10: The Scatter Plot of Calibration Data Points from Calibration Tests Matches a Linear Regression.

in the flume was set to a constant flow, and the probe was held at a constant depth of 2.5 cm. The sensor was started 90 degrees perpendicular to the direction of flow and then rotated into the flow until it was 180 degrees from its starting position as shown in Figure 3.11. This test was repeated twice, once rotating clockwise and once anticlockwise.

The results of this test are shown in Figure 3.12 with the sensor's measurement in blue and a cosine wave in red. The peaks of the sensor values at zero degrees in Figure 3.12 represent the maximum water speed from zero angle difference between sensor orientation and water flow direction. Across multiple tests, the sensor's reduction in measurement corresponds to a cosine function from -75°to 75°. When the sensor is approaching 0°, the measurement is noisier when compared to moving away from 0°, allowing for some sense of direction of rotation. The value the sensor measures approaches zero as the sensor orientation approaches perpendicular to the flow of water. Once reaching perpendicular, the sensor becomes incredibly noisy, resulting in incredibly high positive and negative measurements.

The velocity sensor's readings are reduced by 25% on average when the orientation is

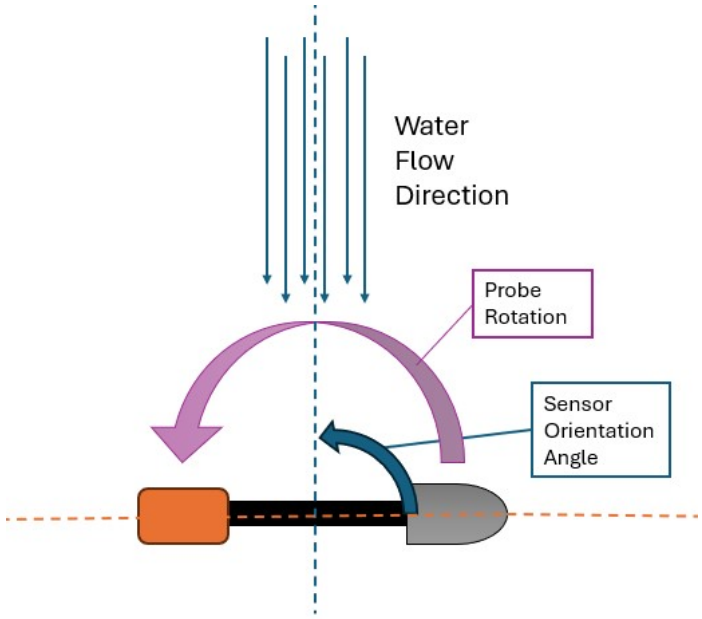

Fig. 3.11: Sensor Orientation Relative to Water Flow Direction was Tested Against Sensor Reading.

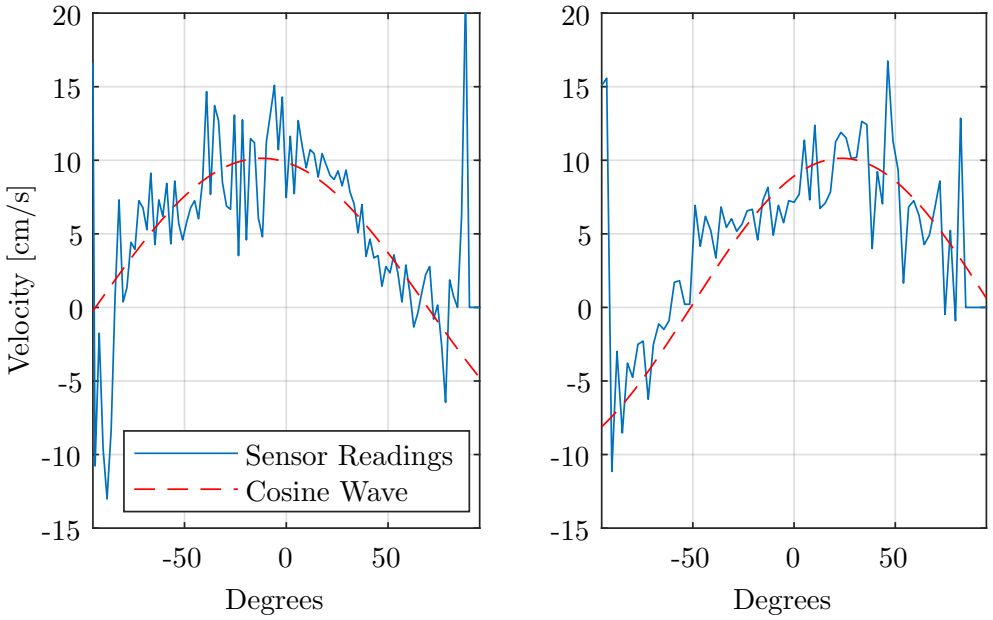

Fig. 3.12: Sensor Reading Against Degree of Orientation During Rotational Test Shows a Cosine Relation.

only 20°misaligned. This increases to a 75% reduction in reading when the orientation is 45°misaligned. The importance of sensor alignment will be shown in the results of field tests. In order to properly align the probe in flight, the UAS must yaw to rotate the probe similarly. Once the probe is aligned with the water flow, it will produce the highest velocity reading. In order to find this reading within a highly noisy data set, the resulting data is passed through a 5-point moving average filter. Then, the maximum value within the data is found. If there are at least 20 other values within 0.061 m/s of that value, then the value is used as the reading. 0.061 m/s represents twice the accuracy range of the EM 950 sensor. The velocity sensor with the manufacturer datalogger has an accuracy of ±1.5 cm/s, but because of the inaccuracies of the UAS, this was increased to ±3.0 cm/s.

3.7 UAS used with Payload

In all flight tests over water, the UAS used was the X4 Standard (Aurelia Aerospace, Las Vegas, NV) shown in Figure 3.13, which was chosen as it met the flight time needed while being relatively inexpensive at under $2000 USD. The payload is mounted underneath the UAS on a pair of rails, and the auxiliary power ports from the UAS power the payload. The aircraft is able to fly with the payload for up to 25 minutes and can resist winds up to 11 m/s, making it ideal for windier and larger coastal channels. It was found during flights with the payload that wind dampened the pendulum swinging of the cable, meaning that moderate winds under 11 m/s can be flown in. The X4 is equipped with ArduPilot allowing for autopilot flight planning and very stable GPS-based position holding, which is important for holding position when measuring.

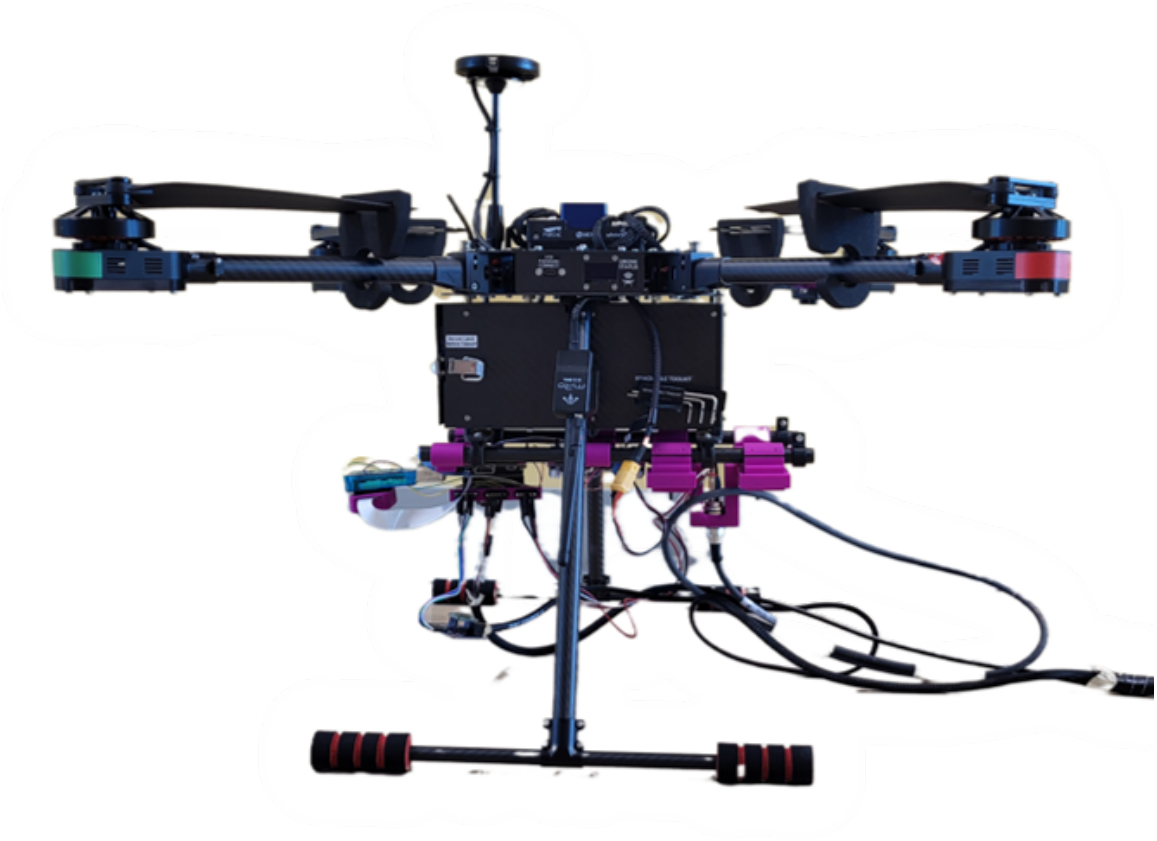

Fig. 3.13: The Aurelia X4 Standard UAS with Payload Mounted Underneath was Flown for Aerial Deployments.

CHAPTER 4

Results

4.1 Field Validation

Once the Raspberry Pi was validated in controlled environments, it needed to be used as a handheld datalogger and with the UAS. Tests in an agricultural canal allow for a comparison between the Raspberry Pi and manufacturer datalogger as a handheld datalogger. Fieldwork in North Carolina tests the payload's ability on a UAS in a tidal channel, which better represents typical aquaculture environments.

4.1.1 Velocity Magnitude Validation: Canal Deployment

To test the payload in a less controlled environment than the UWRL flumes, the payload was tested in an agricultural canal in Logan, Utah, with defined canal geometry. Both the payload and manufacturer datalogger were used to validate the payload. The sensor was attached to an adjustable measuring rod to verify the depth and avoid any disturbances caused by a UAS. The water had a total depth of roughly 14 cm. About every 2 cm from 12 to 4 cm was measured for 30 seconds each. The sensor was held constant in the center of the channel facing into water flow during this time. This was equivalent to about 100 samples from the payload and 50 from the manufacturer datalogger. The sensor readings were significantly noisier with the payload than with the datalogger, likely due to internal filtering within the datalogger. Each depth was filtered with outlier removal and a 9-step moving average filter. The readings from each depth provide a depth profile of the channel provided in Figure 4.1. The profile shows matching results to the manufacturer datalogger with more exaggerated differences within the profile in the payload's results. The manufacturer datalogger measured a mean velocity of 1.245 m/s over the profile. The payload measured a mean velocity of 1.229 m/s. During this test the payload has a mean

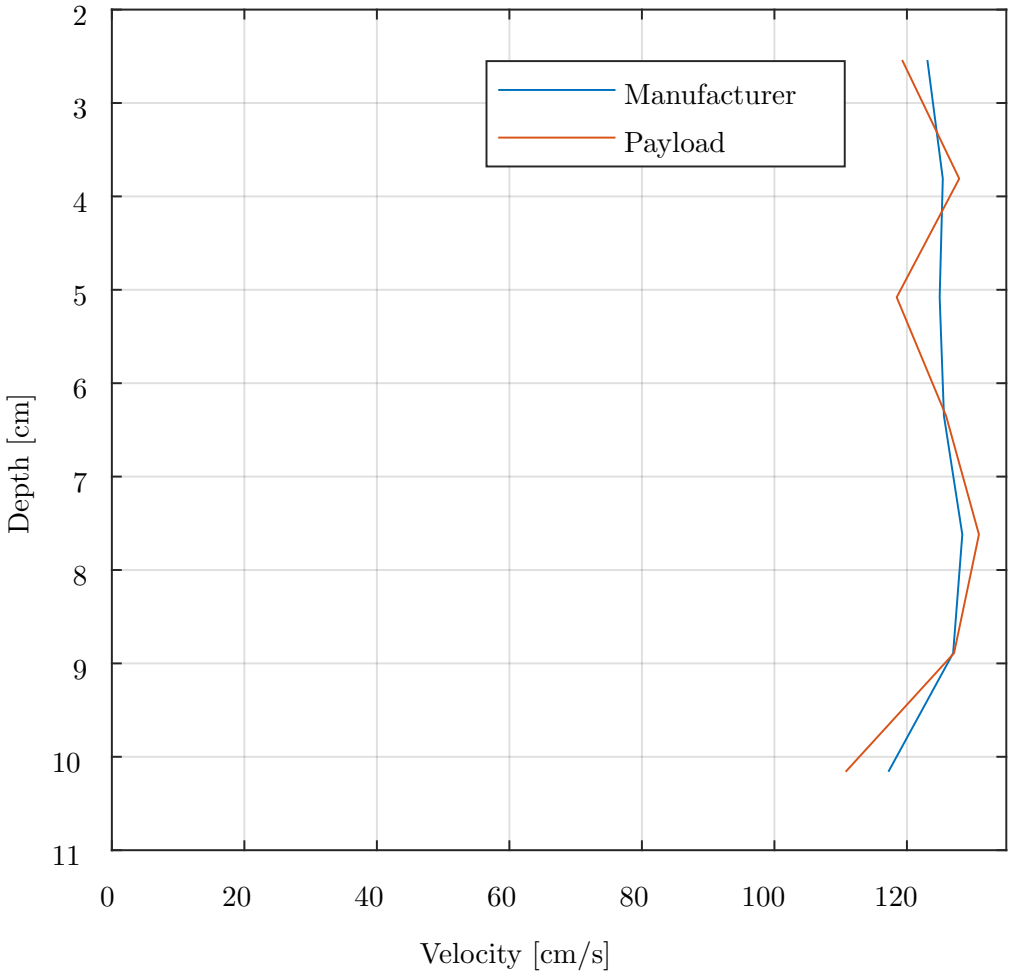

Fig. 4.1: Depth Velocity Profile from Canal Tests with both Manufacturer and Payload Dataloggers Shows Similar Measurements.

absolute error of 10.4% at each depth, however, the mean velocities have nearly identical results with only a mean error of 1.3%. This test verifies the payload as an alternative datalogger to the manufacturer one, showing matching results with an acceptable error.

4.1.2 UAS Field Validation of Probe Rotation

Tests of the payload on a UAS were conducted in a small creek near Logan, UT, in water velocities under 0.3 m/s and depths up to 0.5 m. These tests would verify the ability of the sensor to operate on a UAS and, more specifically, the rotation of the sensor to

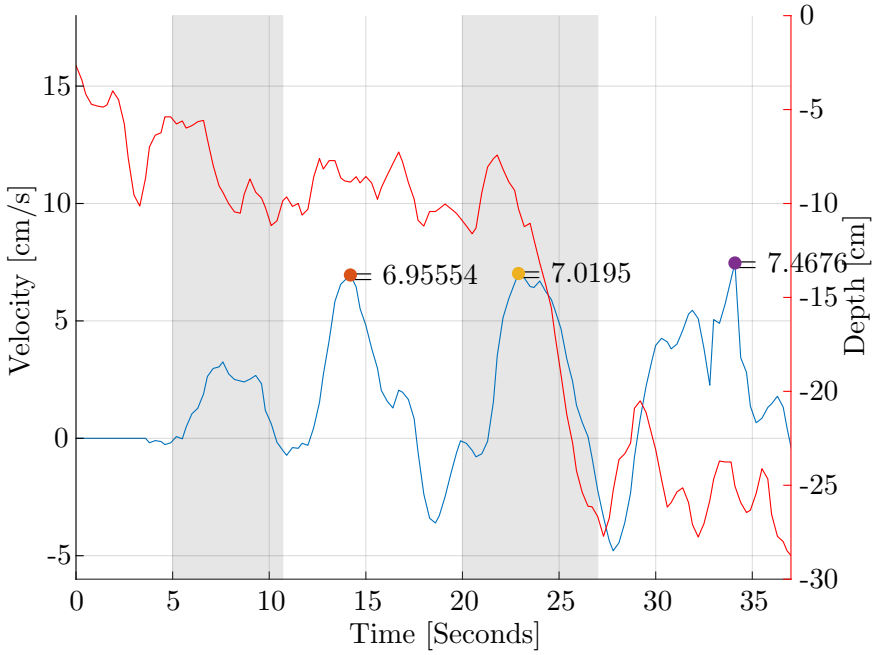

Fig. 4.2: Four Sensor Rotations in a UAS Test Show Water Velocity Changes Due to Orientation of the Probe with Individual Rotations Alternating Shading and No Shading.

capture the highest velocity value. The sensor was attached to a UAS and was placed in the center of the creek. The UAS rotated clockwise to produce a similar rotation in the sensor, completing four total rotations.

The velocity measurements of the test were processed using a 5-step moving average filter and are shown in Figure 4.2. Four periodic oscillations can be seen in Figure 4.2, which each represent one rotation. The individual rotations are alternated in shading and no shading. The peak value was repeatedly measured at 0.07 m/s. The sensor's cable is not rigid, which caused uneven rotation in the probe despite even UAS rotation. The flow of the water quickly rotated the probe when it was perpendicular to the direction of flow, which is why the high-noise perpendicular readings seen in the lab rotation test are not present. The probe was held between 6 cm and 21 cm, with the first rotation being mostly near the surface above 10 cm depth. The shallow measurements have lower recorded velocities because of the sensor's inability to measure surface velocities. This test validates the sensor's ability to capture velocity from rotation in a moving stream.

Fig. 4.3: The Location of the Testing Site is a Channel Near Otway, NC. (Google Images, 2024)

4.2 Field Deployment

The original goal of the payload was to rapidly measure the water velocity of oyster beds and other tidal channels. Fieldwork near Otway, NC, was performed with a team from North Carolina State University. The location was chosen for the large concrete channel with known cross-sectional dimensions and an overhanging bridge. The area also contains oyster beds upstream of the bridge which are within range to be measured. This location and the area of deployment are shown in Figures 4.3 and 4.4.

At the field testing location, the payload was used on both flights and stationary measurements from a bridge over the channel. The bridge measurements were taken because of high winds, resulting in the payload being placed in the water for 1 hour and 10 minutes of consecutive seconds. These measurements were taken alongside an ADCP placed near the sensor and were taken over the changing direction of the tide. Once conditions were favor-

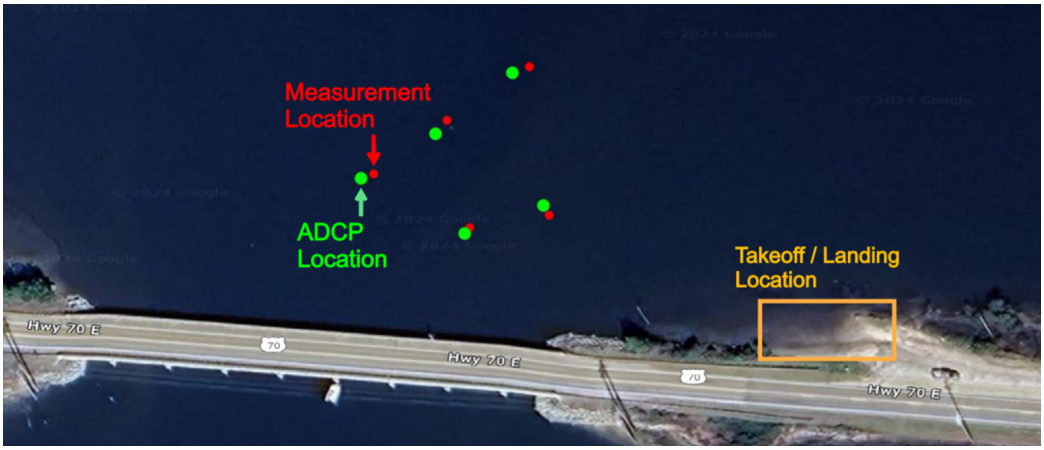

Fig. 4.4: UAS Measurements were taken at the Locations in Red. ADCP Measurements were taken at the Locations in Green (Google Images, 2024).

able, multiple flights were flown, collecting measurements in locations across the channel while being followed by a towed ADCP.

4.2.1 Stationary Deployment: Bridge Test

During the changing of the tide, the payload was placed on a bridge above a concrete channel for 1 hour and 10 minutes. It was able to measure the water velocity alongside a stationary ADCP. The recorded velocity is shown in Figure 4.5 where the velocity reduces to nearly zero, then increases to nearly 15 cm/s. The velocity reaching zero indicates the time when the tide changed direction, at which the sensor was rotated to match the new direction of the tide. The depth of the payload was not varied as frequently when compared to the UAS tests, so a full-depth profile was not available at all times.

The ADCP recorded a full-depth profile, allowing the sensor readings at specific depths to be compared. The measurements of both the ADCP and payload are shown in Figure 4.6. During the period of slowest moving water, the payload was only measuring 3 cm/s when the water was moving 6 cm/s. The payload's sensor was not rigidly attached so it was likely unaligned at this time, when the direction of the water is switching. Once the water velocity increases, the payload was more accurate to the velocities of the ADCP.

It is worth noting in Figure 4.7 that the zero velocity measurements present in several

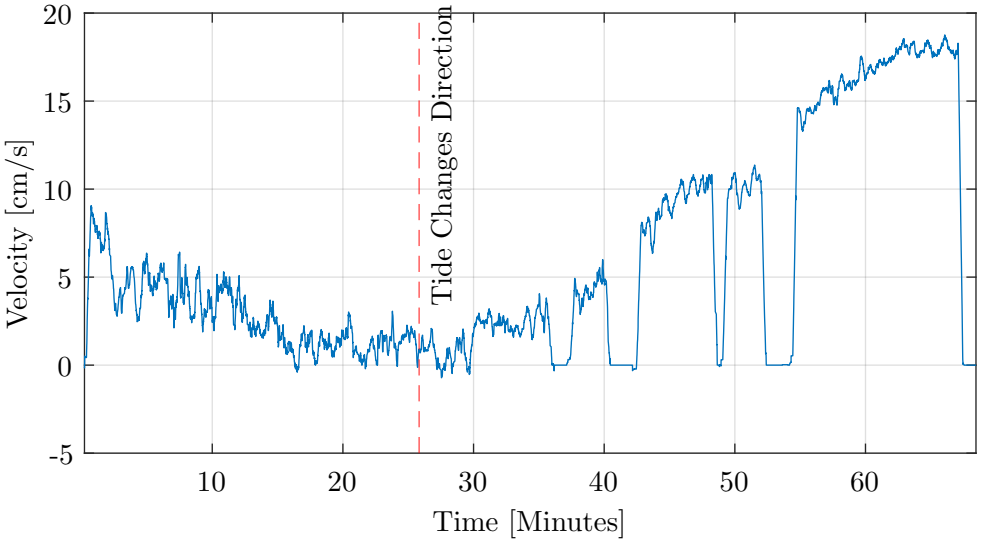

Fig. 4.5: Payload Measurements Shown during the Tide Change shown in Blue.

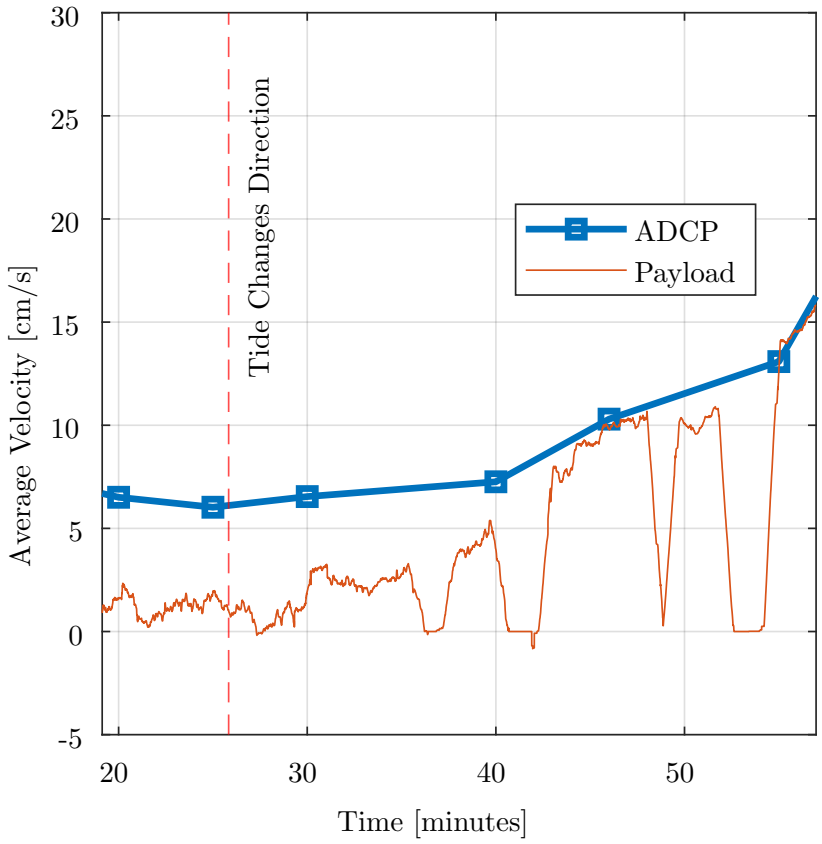

Fig. 4.6: ADCP Velocity Measurements (Blue) were taken alongside the Payload Velocity Measurements (Orange) at the Bridge.

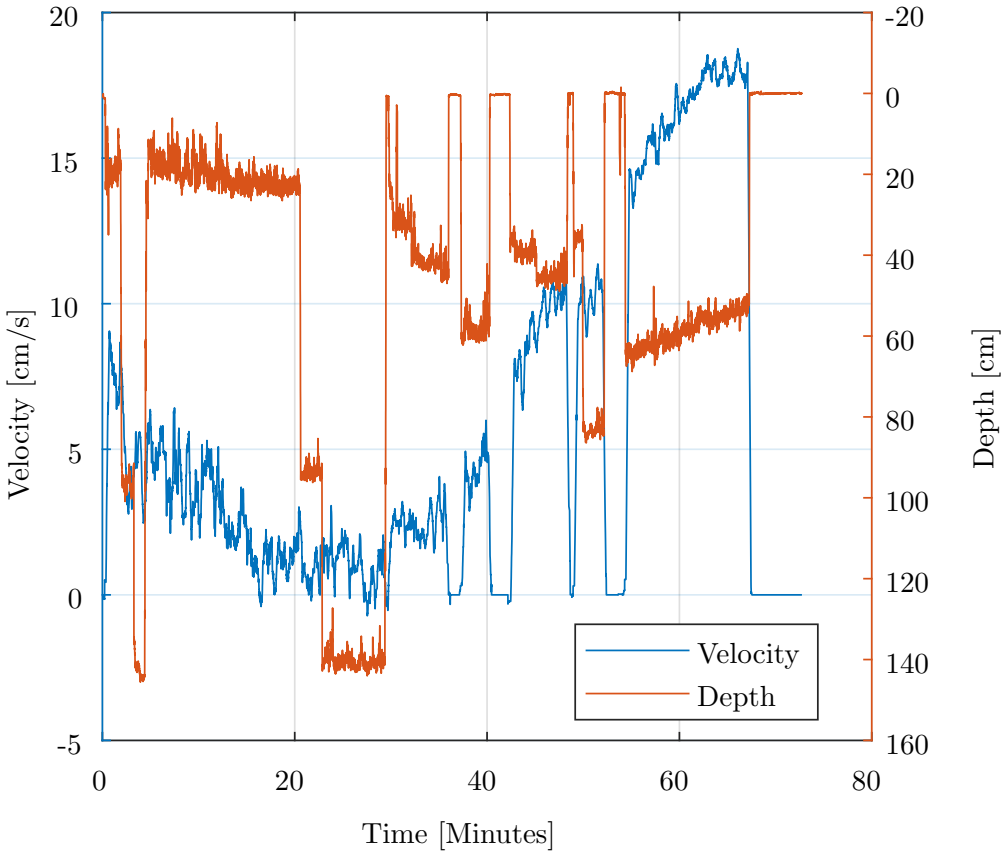

Fig. 4.7: Payload Velocity Measurements (Blue) are much Noisier when Taken near the Surface of the Water as Shown by the Sensor Depth (Orange).

Flight	Measurements Collected
1	6
2	10
3	8
4	13

Table 4.1: Flight-Measurement Breakdown of Field Testing in NC

places are times when the probe was briefly taken out of the water. One notable feature of the readings from the bridge is the difference in sensor noise dependent on depth. The sensor readings are initially very noisy relative to the rest of the data in Figure 4.7. This is the only time where the sensor depth is 20 cm or less. At around 5 minutes, the sensor briefly descends to 1 m depth. At this time, the deviation in sensor readings reduces with the same mean measurement. The standard deviation from the sensor readings while at a depth of 20 cm or less was 4.303 cm/s; between 45 and 70 cm depth, the standard deviation was 2.206 cm/s; and when between 135 and 145 cm depth, the standard deviation was only 2.584 cm/s. The recommended minimum depth for the EM950 sensor is 4.45 cm, much less than the 20 cm range that is experiencing noise. One potential cause for this turbulent surface condition is strong wind passing under the bridge.

4.2.2 Mobile Deployment: UAS Flight Tests

To verify the payload's ability to perform as a rapid aerial measurement platform, the payload was attached to a UAS and flown over the Otway channel. Four flights over two days were flown, collecting measurements as shown in Table 4.1. After arriving at a location, the UAS held a position through GPS hold and then lowered the probe into the water. The UAS carrying the payload was followed by an ADCP, which recorded velocity profiles at the approximate location of the UAS.

At each measurement location, the UAS held a position for roughly one minute, taking measurements from the surface up to 1.3 m deep, emphasizing measuring the 0.3 m to 1 m range. This was achieved through visual markers on the cable that acted as depth indicators for the pilot. Because of UAS drift, the depth varied quickly and often reached the channel

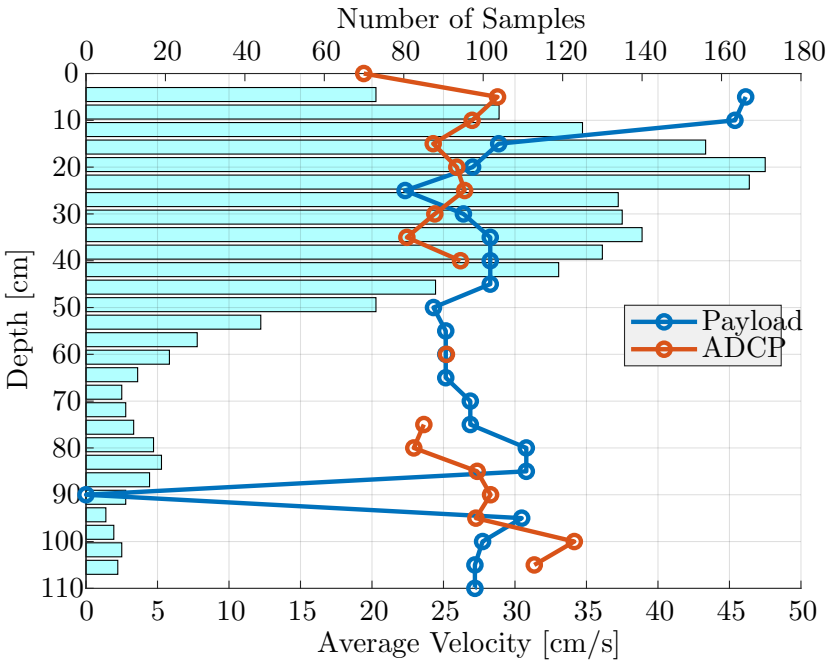

Fig. 4.8: Depth Velocity Profile of Payload (Blue) Compared with ADCP Readings (Orange) with Payload Measurement Sample Count (Light Blue) with Proper Alignment from First Day of Flights

floor. The velocity of the water did not vary temporally enough for vertical drift to become a factor, so recorded measurements could be grouped by depth. The first day of flights had much longer times spent at locations which resulted in profiles with much less variation across depth as shown by Figure 4.8. Comparing the profiles of the payload to the ADCP on the second day, where locations were measured for less time, the payload is more erratic than the ADCP in its measurement, similar to the canal tests previously mentioned. This is evident in Figure 4.9, where the mean velocity is similar, but the variance in readings is much higher.

In another location, the readings are consistently lower by an average of 7 cm/s at all points, as shown in Figure 4.10. This is due to the direction of the probe not being aligned with the direction of water flow, as discussed in Subsection 3.6.2. During each flight, the UAS was yawed several rotations to attempt to rotate the probe a similar amount. However, the water made it difficult to rotate the probe and it is possible the probe did not rotate

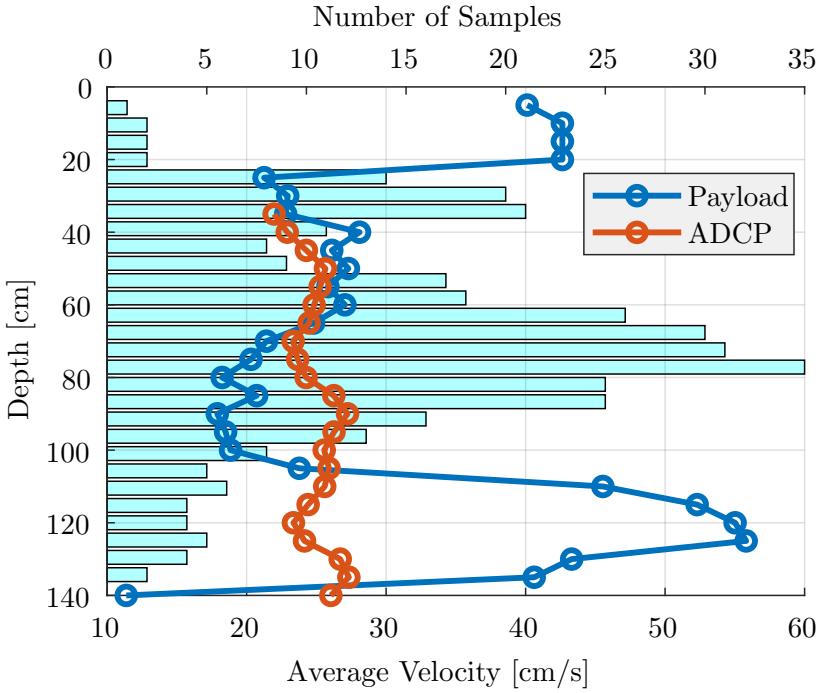

Fig. 4.9: Depth Velocity Profile of Payload (Blue) Compared with ADCP Readings (Orange) with Payload Measurement Sample Count (Light Blue) with Proper Alignment from Second Day of Flights

	Absolute Error	Mean Error
Stationary Canal Measurements	5.5%	2.6%
Stationary Bridge Measurements	10.8%	1.8 %
Flight Depth Velocity Profiles	4.23% to 31.7%	3.89% to 24.4%

Table 4.2: Summary of Errors Across all Days of the Field Testing in Otway, NC.

fully. The ADCP can determine the magnitude of the water velocity but not the direction of water flow.

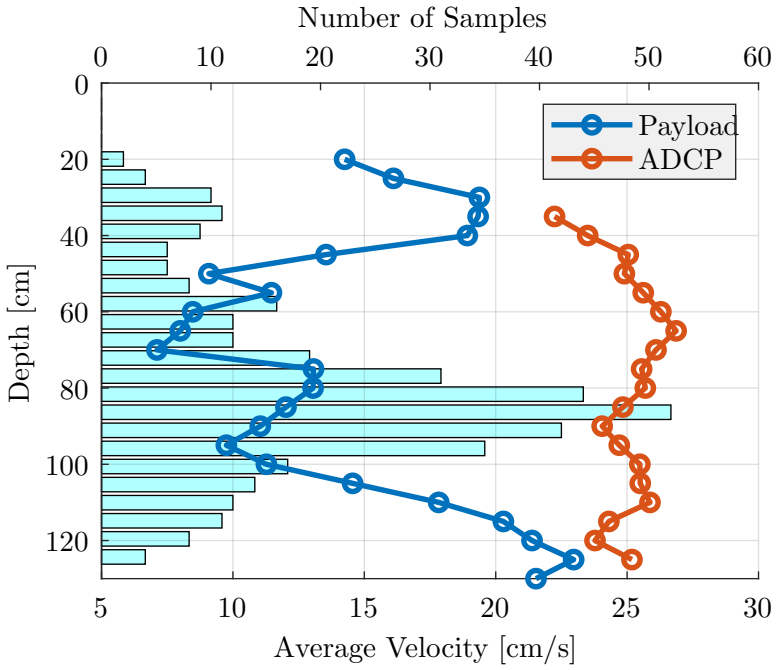

Fig. 4.10: The Depth Velocity Profile of the Payload (Blue) when Misaligned Records Lower Values than the ADCP (Orange).

The results of the payload's performance are shown in Table 4.2. The errors are lowest in the stationary canal measurements where the sensor is fixed in direction, with only a slight increase in the stationary measurements from the bridge. The absolute error present in both could be reduced through better filtering in the payload, and the mean error was low enough for the payload to work as a standalone sensor. The flights had more overall error, with a wide range of errors across the profiles. The errors are caused by poor control of the probe, resulting in misalignment at some depths. Additional profiles are shown in Figure (4.11) and in the appendix in Figure (A.2) and Figure (A.1), where the tendency for higher error at lower sample count is present.

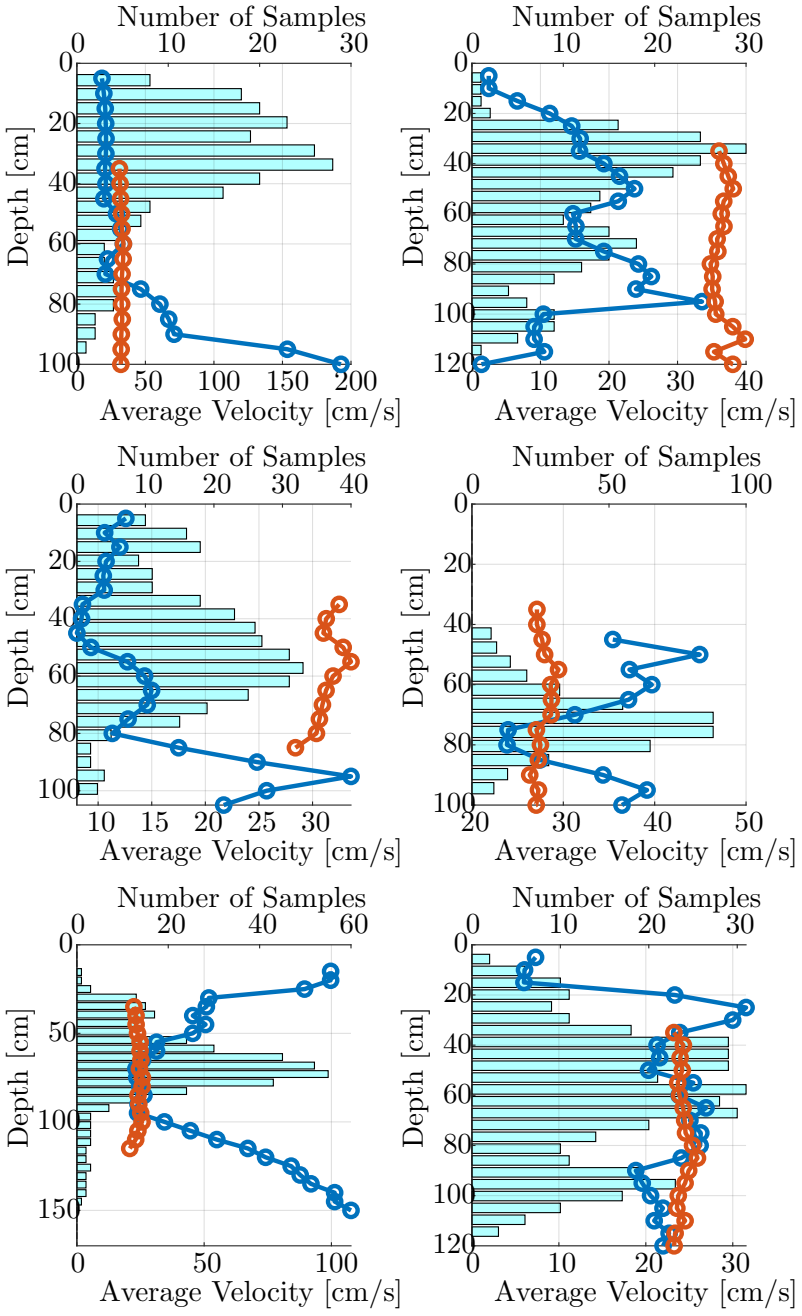

Fig. 4.11: Depth Velocity Profiles with Payload Velocities (Blue), ADCP Velocities (Orange), and Payload Sample Count (Light Blue). Depths with Lower Sample Counts have Less Accuracy when Compared to the ADCP. Other Plots have Consistently Lower Values from Probe Misalignment.

CHAPTER 5

Discussion

The tests performed have shown the strengths and weaknesses of the payload based on several factors. The payload was tested against current velocity measurements in a natural oyster lease. The problem of probe angle was present in every UAS deployed test and severely lowered the values. Probe performance was best in the middle depths of measurement due primarily to a higher number of samples. The sensor did have a higher amount of noise than other velocity measurement methods, especially at shallower depths. The payload deployment alongside an ADCP allowed for comparing deployment times, in which the payload and UAS were significantly faster than ADCPs. Based on these reasons, the payload presents a new rapid method for subsurface velocity measurement in aquaculture farms.

5.1 Effects of Probe Angle

When attempting to take measurements in the field, it was obvious that some velocity measurements were consistently lower than the ADCP's validated measurements. This decrease was not consistent among all measurement locations throughout a single flight, meaning that the decrease was not from an error in the payload throughout that flight. The decrease in velocity based on probe angle relative to the water flow direction was observed in lab tests with similar effects to those observed in the field flights. It is also known for some of the tests that the probe entered the water in the wrong orientation. Therefore, it is safe to assume that the lower measurements are from the misaligned probe.

The cause of probe misalignment is the non-rigid cable the probe is attached with. Without a rigid mount, the probe angle can't be directly tied to the direction of the UAS. Additionally, the water made it difficult to move the probe because of how little for can be applied through the cable.

In field tests, the rotation of the UAS did rotate the probe, allowing for the probe to move through a wide range of values around the direction of flow. This correction helped several locations capture the correct velocity compared to the ADCP. However, these rotations added more time to measuring a location's depth velocity profile. This is because rather than rotating at the same rate as the UAS, the cable will twist before rotating the probe, causing the probe to rotate slower. More time spent on UAS movement limits the number of locations that can be measured in a single flight.

5.2 Mid-Depth Performance

The best-performing range of values on a depth velocity profile is often the middle range of depths. It is common for in-situ water velocity sources to perform poorly or not at all at shallow depths and the surface. The ADCPs used during field testing cannot measure velocities between the surface and 30 cm underneath the surface. This same range of depths often had the least amount of samples collected by the payload because of a focus on the 0.3 m to 1 m range of depths. When the sensor collects fewer samples in the middle range, it often results in inaccurate velocity measurements, as demonstrated by Figure 5.1.

During tests, the floor of the channel also suffered from low samples because The EM950 sensor is not able to measure when it contacts a solid surface. This causes the sensor to measure a constant zero m/s when it reaches the floor of a water body which skews the data to be lower at this region.

Compared to the ADCP results, the bottom and top regions had significantly more error than the middle region as shown in Table 5.1. The error was consistently at least 10% higher than the middle region. This does include poorly aligned profiles, but the error trend was still present among more well-aligned profiles. This error is found among flight tests during the field campaign and does not include stationary tests. This data also does not include measurements where the sensor hit the floor of the channel, which would have further lowered the value of the error.

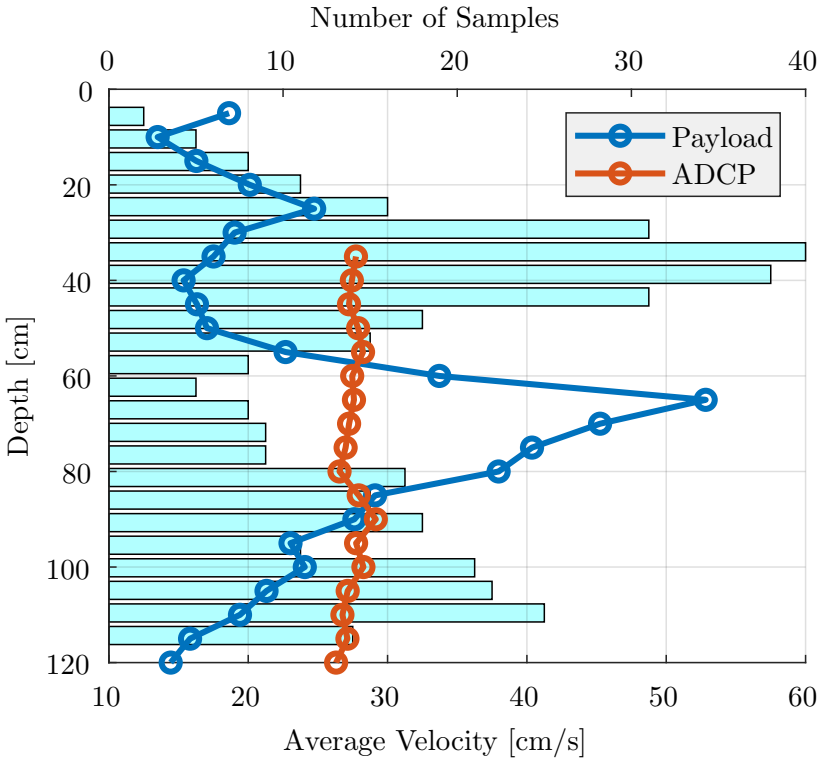

Fig. 5.1: Poor Sample Distribution (Light Blue) of Payload Measurements (Blue) Misrepresents the Actual Velocity Profile Measured by the ADCP (Orange).

Depth	Mean Error
Top 20%	44.8%
Middle 60%	29.0%
Bottom 20%	39.2%

Table 5.1: The Velocity Profile Errors are Higher at the Surface and Floor of the Channel.

5.3 UAS Drift

An initial concern with the payload was the effect UAS drift would have on sensor reading. The sensor measures water velocity assuming it is stationary, so any movement in the UAS would result in the sensor reading a relative velocity, which is a combination of water and UAS velocities. However, the UAS used in tests held its lateral position within 50 cm/s of its center point in winds up to 7 m/s. Slack in the cable also allowed the probe to remain stationary despite small movements in the UAS, so the probe never experienced movement laterally because of the UAS.

5.4 Sensor Noise

When compared to the ADCP or the Hach datalogger, the sensor presented much noisier data. This is because the datalogger that the sensor is typically used with applies a running average filter. For the static bridge test a running average filter is used to smooth the data, however, this cannot be used for UAS depth velocity profiles. This is because the UAS drifts vertically during measurement, and a running average filter would average data from a range of depths. Instead, the data must be sorted by depth first, then outliers removed, and then a common maximum value found.

Another source of noise in the sensor was in shallow velocity measurements. In the static field tests, results from 0 to 20 cm depth had twice the standard deviation of the rest of the measurements below 20 cm. EMVs typically can't measure surface velocities because they rely on a volume of water around the sensor, which is also why they struggle in shallow velocities.

5.5 Human Factors

The purpose of the project is to increase the sensor deployment speed to collect more samples across more locations than current aquaculture sensing methods are able to. The field tests in Otway resembled the actual deployment of the payload into coastal oyster beds. Being conducted alongside multiple ADCPs allowed a direct comparison against a standard velocity measurement technique in a proper environment.

The ADCPs had four or more people who initialized, deployed, and monitored the sensor during its deployment. Often, over thirty minutes were needed to set up the ADCP, and over ten minutes were needed to move it onto the water and anchor it in place. Comparatively, the UAS and payload only ever had one person who both set up and flew the drone. The UAS could be unboxed and calibrated in under two minutes, and the payload could be mounted in under a minute. Over the course of a dozen flights, the time between site arrival and UAS takeoff was as low as eight minutes, with an average of around 11 minutes. This is already an improvement over the ADCP which is additionally stationary or slowly moved by a kayak. The UAS could be made even faster with the use of autopilot software to fly autonomously, as during field tests, the pilot would have to move from the takeoff location to a location with better visibility or perspective.

5.6 Payload Performance

After performing field testing it is clear that the payload has succeeded at rapidly measuring water velocity. From field tests, the mean error of the sensor was between 4.1% and 31.7% of ADCP readings. This error includes profiles that included sensor misalignment evident from a constant velocity offset. With proper alignment and a moving average filter, the error can be reduced to 2.58%, as shown in stationary tests. For a stand-alone scientific instrument, this error would be much too high for use, however, it is important to consider the goal of the payload is rapid measurement above highly accurate measurement.

CHAPTER 6

Conclusions

Rapid remote depth velocity profile measurement techniques for water channels do not currently exist. The aquaculture industry primarily relies on stationary sensors or infrequent sensing, which creates data sets with spatial and temporal gaps. This payload contributes to the field of hydrology by providing a rapid depth velocity profile measurement method. The developed payload is able to quickly deploy on a UAS and measure ten or more depth velocity profiles on a single flight. Deployment times for the payload are, on average, ten minutes, which is much lower than ADCP or MSV deployment times, resulting in faster data collection and less time between measurement sites. The sensors are able to get a good first measurement of water velocity in an area which informs whether additional, more precise sensing is needed by other industry standard methods.

The payload was designed with an industry-standard sensor for velocity. The EM950 velocity sensor was selected because of its electromagnetic operating principle and low weight. The sensor's communication was reverse-engineered for use on a UAS and with a different datalogger. Controlled tests against the intended datalogger in a controlled water flume verified the Raspberry Pi as an alternate datalogger. Testing from 0 m/s to 1.5 m/s in 10 cm/s increments confirmed the first-order calibration curve needed to convert the sensor's unitless results into m/s. Additional tests identified the effect of sensor orientation relative to water flow direction on the accuracy of velocity measurement.

Canal tests validated the payload as an alternate datalogger in a common environment where the sensor is used in hydrology. Compared to the intended datalogger, the payload had a mean error of 2.58% when properly aligned to the flow direction. The payload was designed with a magnetic release that prevents it from becoming a danger to its UAS without releasing the sensors unintentionally. Once the payload was validated in stationary tests, it was deployed on a UAS in several tests in small streams which verified its ability

as a UAS payload to measure water velocity.

During fieldwork in Otway, North Carolina, the payload was tested in one day of static deployment and two days of flights. An ADCP provided ground truth water velocity measurements for the payload during all three days. The static measurement was over an hour of measurement near the center of a concrete channel. This provided a measurement of the changing of the direction of tide within 1.8% of the ADCP's measurements. The results demonstrated the effect of depth on sensor signal noise where readings within the first 20 cm have double the standard deviation of deeper results. The first day of flights measured a transect of the channel, demonstrating the payload's ability to make the depth velocity profile of a channel cross-section. On the second day of flights, the depth velocity profiles were measured at as many points in the area as possible on each flight. This simulated the use of the payload in aquaculture farms for rapid sensing over an area. Each depth velocity profile was measured within two minutes of reaching the location with travel time being relatively low when compared to MSV deployment. The payload's measurements sometimes suffered from probe misalignment, resulting in mean errors between 4% and 31% of nearby ADCP measurements. ADCP deployment was much slower than the UAS's total deployment, confirming the payload's ability to improve the speed of coastal water velocity measurement. This payload has demonstrated the ability to quickly characterize water velocities over large areas, which can be used to inform further use of more precise sensors.

6.1 Future Work

The payload had three main problems found in testing:

1. A lack of surface water velocity data collection
2. Vertical UAS drift causing poor sample distribution
3. Orientation misalignment providing inaccurate measurements

The payload was not able to measure the surface properly, so an easy solution would be to combine the payload with a PIV camera. This is tested technology and the work would be primarily in combining the data between surface maps and in-situ vertical profiles.

To guarantee a certain amount of samples at each depth, the payload can also be further automated with precise depth control as done in Ore et al. [37]. Depth control combined with better orientation control could reduce the time needed to measure a location.

The largest problem the payload has is the effect of misalignment on the sensor's measurement. The current method to deal with this is to rotate the UAS which is inconsistent, slow, and does not guarantee the sensor reaches the correct orientation. One solution that was attempted was fins on the probe which would align the probe to the flow direction. This did not work because of the low velocities in which the probe was tested. A rigid linking between the probe and the UAS was also considered but not used because of difficulty in flying and weight. A solution to the problem is to actively control the rotation of the probe with a motorized tail propeller. Mounting this to the tail end of the probe provides better control over its orientation. This could be automated to sweep for the largest velocity reading and remain at that orientation.

REFERENCES

[1] D. Klinger and R. Naylor, "Searching for solutions in aquaculture: Charting a sustainable course," *Annual Review of Environment and Resources*, vol. 37, no. Volume 37, 2012, pp. 247–276, 2012. [Online]. Available: https://www.annualreviews.org/content/journals/10.1146/annurev-environ-021111-161531

[2] E. Garel, S. Nunes, J. M. Neto, R. Fernandes, R. Neves, J. Marques, and O. Ferreira, "The autonomous simpatico system for real-time continuous water-quality and current velocity monitoring: Examples of application in three portuguese estuaries," *Geo-Marine Letters*, vol. 29, pp. 331–341, 10 2009.

[3] S. Pearce, R. Ljubičić, S. Peña-Haro, M. Perks, F. Tauro, A. Pizarro, S. F. Dal Sasso, D. Strelnikova, S. Grimaldi, I. Maddock, G. Paulus, J. Plavšić, D. Prodanović, and S. Manfreda, "An evaluation of image velocimetry techniques under low flow conditions and high seeding densities using unmanned aerial systems," *Remote Sensing*, vol. 12, no. 2, 2020. [Online]. Available: https://www.mdpi.com/2072-4292/12/2/232

[4] L. Cao, W. Wang, Y. Yang, C. Yang, Z. Yuan, S. Xiong, and J. Diana, "Environmental impact of aquaculture and countermeasures to aquaculture pollution in china," *Environmental science and pollution research international*, vol. 14, pp. 452–62, 12 2007.

[5] L. Parra, G. Lloret, J. Lloret, and M. Rodilla, "Physical sensors for precision aquaculture: A review," *IEEE Sensors Journal*, vol. 18, no. 10, pp. 3915–3923, 2018.

[6] D. Ivetić, D. Prodanović, and L. Stojadinović, "Bed-mounted electro magnetic meters: Implications for robust velocity measurement in urban drainage systems," *Journal of Hydrology*, vol. 566, pp. 455–469, 2018. [Online]. Available: https://www.sciencedirect.com/science/article/pii/S0022169418306711

[7] J. Sun, L. Zhang, G. Tu, S. Zhen, Z. Cao, G. Zhang, and B. Yu, "Laser velocimetry for the in situ sensing of deep-sea hydrothermal flow velocity," *Sensors*, vol. 23, no. 20, 2023. [Online]. Available: https://www.mdpi.com/1424-8220/23/20/8411

[8] J.-Y. Lin, H.-L. Tsai, and W.-H. Lyu, "An integrated wireless multi-sensor system for monitoring the water quality of aquaculture," *Sensors*, vol. 21, no. 24, 2021. [Online]. Available: https://www.mdpi.com/1424-8220/21/24/8179

[9] A. U. Alam, D. Clyne, H. Jin, N.-X. Hu, and M. J. Deen, "Fully integrated, simple, and low-cost electrochemical sensor array for in situ water quality monitoring," *ACS Sensors*, vol. 5, no. 2, pp. 412–422, 2020, pMID: 32028771. [Online]. Available: https://doi.org/10.1021/acssensors.9b02095

[10] K. Oberg and D. S. Mueller, "Validation of streamflow measurements made with acoustic doppler current profilers," *Journal of Hydraulic Engineering*, vol. 133, no. 12, pp. 1421–1432, 2007. [Online]. Available: https://ascelibrary.org/doi/abs/10.1061/%28ASCE%290733-9429%282007%29133%3A12%281421%29

[11] M. Simpson and R. Bland, "Methods for accurate estimation of net discharge in a tidal channel," *IEEE Journal of Oceanic Engineering*, vol. 25, no. 4, pp. 437–445, 2000.

[12] C. Li, J. Blanton, and C. Chen, "Mapping of tide and tidal flow fields along a tidal channel with vessel-based observations," *Journal of Geophysical Research: Oceans*, vol. 109, no. C4, 2004. [Online]. Available: https://agupubs.onlinelibrary.wiley.com/doi/abs/10.1029/2003JC001992

[13] A. J. F. Hoitink, F. A. Buschman, and B. Vermeulen, "Continuous measurements of discharge from a horizontal acoustic doppler current profiler in a tidal river," *Water Resources Research*, vol. 45, no. 11, 2009. [Online]. Available: https://agupubs.onlinelibrary.wiley.com/doi/abs/10.1029/2009WR007791

[14] M. Muste, K. Yu, and M. Spasojevic, "Practical aspects of adcp data use for quantification of mean river flow characteristics; part i: moving-vessel measurements,"

Flow Measurement and Instrumentation, vol. 15, no. 1, pp. 1–16, 2004. [Online]. Available: https://www.sciencedirect.com/science/article/pii/S0955598603000670

[15] M. Guerra, A. E. Hay, R. Karsten, G. Trowse, and R. A. Cheel, "Turbulent flow mapping in a high-flow tidal channel using mobile acoustic doppler current profilers," *Renewable Energy*, vol. 177, pp. 759–772, 2021. [Online]. Available: https://www.sciencedirect.com/science/article/pii/S0960148121008168

[16] M. Guerrero, N. Rüther, and R. Szupiany, "Laboratory validation of acoustic doppler current profiler (adcp) techniques for suspended sediment investigations," *Flow Measurement and Instrumentation*, vol. 23, no. 1, pp. 40–48, 2012. [Online]. Available: https://www.sciencedirect.com/science/article/pii/S0955598611001038

[17] V. Weitbrecht, G. Kühn, and G. Jirka, "Large scale piv-measurements at the surface of shallow water flows," *Flow Measurement and Instrumentation*, vol. 13, no. 5, pp. 237–245, 2002. [Online]. Available: https://www.sciencedirect.com/science/article/pii/S0955598602000596

[18] W. J. Plant, R. Branch, G. Chatham, C. C. Chickadel, K. Hayes, B. Hayworth, A. Horner-Devine, A. Jessup, D. A. Fong, O. B. Fringer, S. N. Giddings, S. Monismith, and B. Wang, "Remotely sensed river surface features compared with modeling and in situ measurements," *Journal of Geophysical Research: Oceans*, vol. 114, no. C11, 2009. [Online]. Available: https://agupubs.onlinelibrary.wiley.com/doi/abs/10.1029/2009JC005440

[19] W.-C. Liu, C.-H. Lu, and W.-C. Huang, "Large-scale particle image velocimetry to measure streamflow from videos recorded from unmanned aerial vehicle and fixed imaging system," *Remote Sensing*, vol. 13, no. 14, 2021. [Online]. Available: https://www.mdpi.com/2072-4292/13/14/2661

[20] P. Zamankhan, "Large eddy simulation and piv experiments of air–water mixing tanks," *Communications in Nonlinear Science and Numerical Simulation*, vol. 15,

no. 6, pp. 1511–1525, 2010. [Online]. Available: https://www.sciencedirect.com/science/article/pii/S1007570409003591

[21] T. Jin and Q. Liao, "Application of large scale piv in river surface turbulence measurements and water depth estimation," *Flow Measurement and Instrumentation*, vol. 67, pp. 142–152, 2019. [Online]. Available: https://www.sciencedirect.com/science/article/pii/S095559861830133X

[22] M. Vélez-Nicolás, S. García-López, L. Barbero, V. Ruiz-Ortiz, and Sánchez-Bellón, "Applications of unmanned aerial systems (uass) in hydrology: A review," *Remote Sensing*, vol. 13, no. 7, 2021. [Online]. Available: https://www.mdpi.com/2072-4292/13/7/1359

[23] B. S. Acharya, M. Bhandari, F. Bandini, A. Pizarro, M. Perks, D. R. Joshi, S. Wang, T. Dogwiler, R. L. Ray, G. Kharel, and S. Sharma, "Unmanned aerial vehicles in hydrology and water management: Applications, challenges, and perspectives," *Water Resources Research*, vol. 57, no. 11, p. e2021WR029925, 2021, e2021WR029925 2021WR029925. [Online]. Available: https://agupubs.onlinelibrary.wiley.com/doi/abs/10.1029/2021WR029925

[24] *Development and Testing of an Unmanned Aerial Vehicle for Large Scale Particle Image Velocimetry*, ser. Dynamic Systems and Control Conference, vol. Volume 3: Industrial Applications; Modeling for Oil and Gas, Control and Validation, Estimation, and Control of Automotive Systems; Multi-Agent and Networked Systems; Control System Design; Physical Human-Robot Interaction; Rehabilitation Robotics; Sensing and Actuation for Control; Biomedical Systems; Time Delay Systems and Stability; Unmanned Ground and Surface Robotics; Vehicle Motion Controls; Vibration Analysis and Isolation; Vibration and Control for Energy Harvesting; Wind Energy, 10 2014.

[25] C. Chen, D. Liang, X. Wang, and Z. Li, "Application of uav-based piv to rivers," in *2021 7th International Conference on Hydraulic and Civil Engineering & Smart Water*

Conservancy and Intelligent Disaster Reduction Forum (ICHCE & SWIDR), 2021, pp. 1707–1712.

[26] A. Eltner, D. Mader, N. Szopos, B. Nagy, J. Grundmann, and L. Bertalan, "Using thermal and rgb uav imagery to measure surface flow velocities of rivers," *The International Archives of the Photogrammetry, Remote Sensing and Spatial Information Sciences*, vol. XLIII-B2-2021, pp. 717–722, 2021. [Online]. Available: https://isprs-archives.copernicus.org/articles/XLIII-B2-2021/717/2021/

[27] S. J. Dugdale, J. Klaus, and D. M. Hannah, "Looking to the skies: Realising the combined potential of drones and thermal infrared imagery to advance hydrological process understanding in headwaters," *Water Resources Research*, vol. 58, no. 2, p. e2021WR031168, 2022, e2021WR031168 2021WR031168. [Online]. Available: https://agupubs.onlinelibrary.wiley.com/doi/abs/10.1029/2021WR031168

[28] C. Masafu, R. Williams, X. Shi, Q. Yuan, and M. Trigg, "Unpiloted aerial vehicle (uav) image velocimetry for validation of two-dimensional hydraulic model simulations," *Journal of Hydrology*, vol. 612, p. 128217, 2022. [Online]. Available: https://www.sciencedirect.com/science/article/pii/S0022169422007892

[29] I. Fairley, B. J. Williamson, J. McIlvenny, N. King, I. Masters, M. Lewis, S. Neill, D. Glasby, D. Coles, B. Powell, K. Naylor, M. Robinson, and D. E. Reeve, "Drone-based large-scale particle image velocimetry applied to tidal stream energy resource assessment," *Renewable Energy*, vol. 196, pp. 839–855, 2022. [Online]. Available: https://www.sciencedirect.com/science/article/pii/S0960148122009983

[30] I. Fairley, N. King, J. McIlvenny, M. Lewis, S. Neill, B. J. Williamson, I. Masters, and D. E. Reeve, "Intercomparison of surface velocimetry techniques for drone-based marine current characterization," *Estuarine, Coastal and Shelf Science*, vol. 299, p. 108682, 2024. [Online]. Available: https://www.sciencedirect.com/science/article/pii/S0272771424000696

[31] X. Han, K. Chen, Q. Zhong, Q. Chen, F. Wang, and D. Li, "Two-dimensional space-time image velocimetry for surface flow field of mountain rivers based on uav video," *Frontiers in Earth Science*, vol. 9, 2021. [Online]. Available: https://www.frontiersin.org/journals/earth-science/articles/10.3389/feart.2021.686636

[32] P. Koutalakis, M. D. Stamataki, and O. Tzoraki, "Uav-based optical methods to estimate the flow of temporary streams and evaluate their environmental status," *Preprints*, June 2023. [Online]. Available: https://doi.org/10.20944/preprints202306.0768.v1

[33] P. Koutalakis, O. Tzoraki, and G. Zaimes, "Uavs for hydrologic scopes: Application of a low-cost uav to estimate surface water velocity by using three different image-based methods," *Drones*, vol. 3, no. 1, 2019. [Online]. Available: https://www.mdpi.com/2504-446X/3/1/14

[34] K. Song, A. Brewer, S. Ahmadian, A. Shankar, C. Detweiler, and A. J. Burgin, "Using unmanned aerial vehicles to sample aquatic ecosystems," *Limnology and Oceanography: Methods*, vol. 15, no. 12, pp. 1021–1030, 2017. [Online]. Available: https://aslopubs.onlinelibrary.wiley.com/doi/abs/10.1002/lom3.10222

[35] C. Koparan, A. B. Koc, C. V. Privette, and C. B. Sawyer, "In situ water quality measurements using an unmanned aerial vehicle (uav) system," *Water*, vol. 10, no. 3, 2018. [Online]. Available: https://www.mdpi.com/2073-4441/10/3/264

[36] M. Chung, C. Detweiler, M. Hamilton, J. Higgins, J.-P. Ore, and S. Thompson, "Obtaining the thermal structure of lakes from the air," *Water*, vol. 7, pp. 6467–6482, 11 2015.

[37] J.-P. Ore and C. Detweiler, "Sensing water properties at precise depths from the air," *Journal of Field Robotics*, vol. 35, no. 8, pp. 1205–1221, 2018. [Online]. Available: https://onlinelibrary.wiley.com/doi/abs/10.1002/rob.21807

[38] C. Koparan, A. B. Koc, C. V. Privette, C. B. Sawyer, and J. L. Sharp, "Evaluation of a uav-assisted autonomous water sampling," *Water*, vol. 10, no. 5, 2018. [Online]. Available: https://www.mdpi.com/2073-4441/10/5/655

[39] D. A. S. E. A. B. Carrick Detweiler, John-Paul Ore and A. Lorenz, "Environmental reviews and case studies: Bringing unmanned aerial systems closer to the environment," *Environmental Practice*, vol. 17, no. 3, pp. 188–200, 2015. [Online]. Available: https://doi.org/10.1017/S1466046615000174

[40] C. Koparan, A. B. Koc, C. V. Privette, and C. B. Sawyer, "Autonomous in situ measurements of noncontaminant water quality indicators and sample collection with a uav," *Water*, vol. 11, no. 3, 2019. [Online]. Available: https://www.mdpi.com/2073-4441/11/3/604

[41] H. Doi, Y. Akamatsu, Y. Watanabe, M. Goto, R. Inui, I. Katano, M. Nagano, T. Takahara, and T. Minamoto, "Water sampling for environmental dna surveys by using an unmanned aerial vehicle," *Limnology and Oceanography: Methods*, vol. 15, no. 11, pp. 939–944, 2017. [Online]. Available: https://aslopubs.onlinelibrary.wiley.com/doi/abs/10.1002/lom3.10214

[42] A. DeMario, P. Lopez, E. Plewka, R. Wix, H. Xia, E. Zamora, D. Gessler, and A. Yalin, "Water plume temperature measurements by an unmanned aerial system (uas)," *Sensors*, vol. 17, p. 306, 02 2017.

APPENDIX

The following data are the remaining velocity depth profiles from the Otway Field Work. The first profiles do not have an ADCP profile for comparison. Note that when the velocity is measured at zero, it is because there are too few measurements at that depth for a confident measurement. Additionally, some depths appear identical to their neighboring depths. This is because each depth is an average of the surrounding depths so they likely used the same or similar data points.

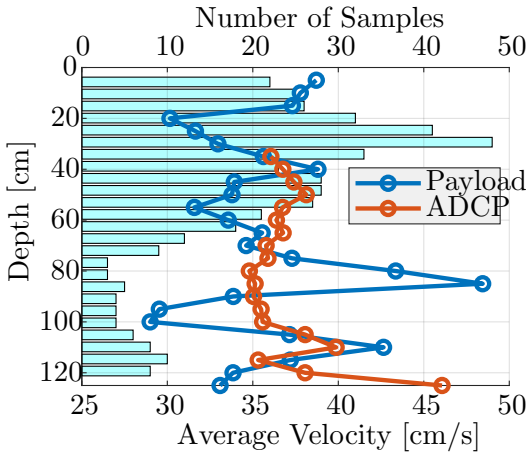

(a) Latitude 34.7812, Longitude -76.5738

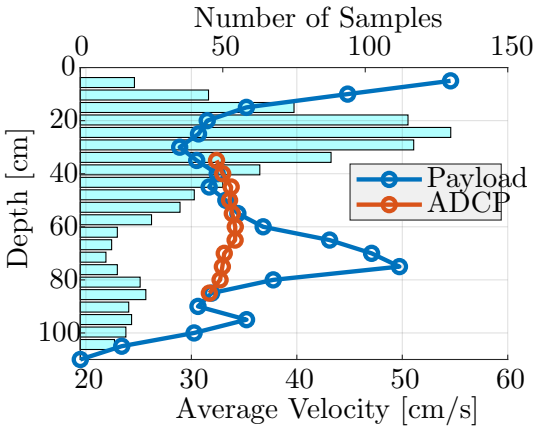

(b) Latitude 34.7811, Longitude -76.5733

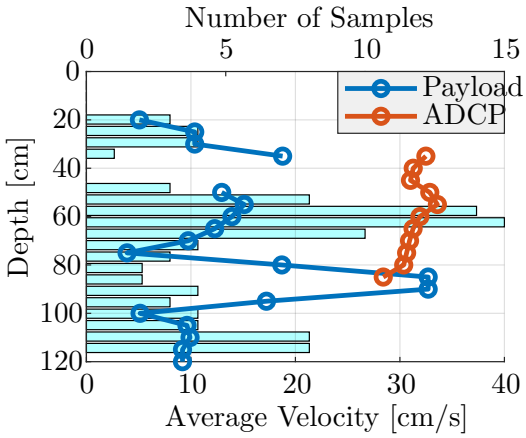

(c) Latitude 34.7813, Longitude -76.5736

Fig. A.1: March 16th, Velocity Profiles

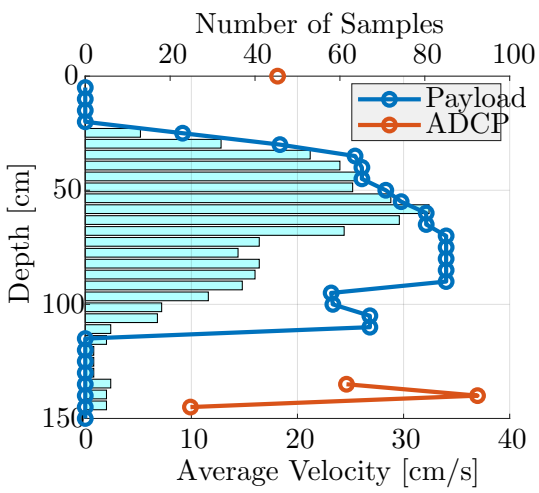

(a) Latitude 34.7809, Longitude -76.5738

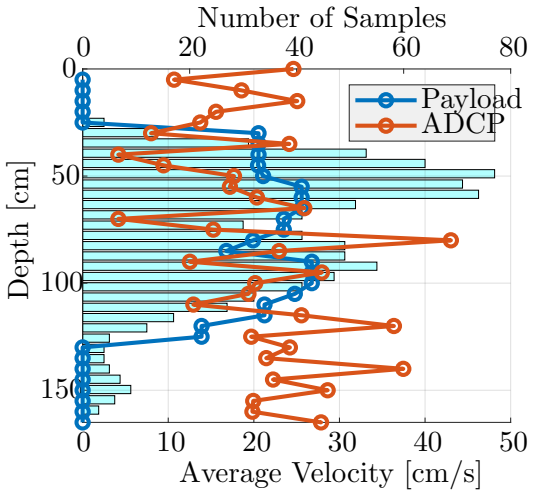

(b) Latitude 34.7809, Longitude -76.5739

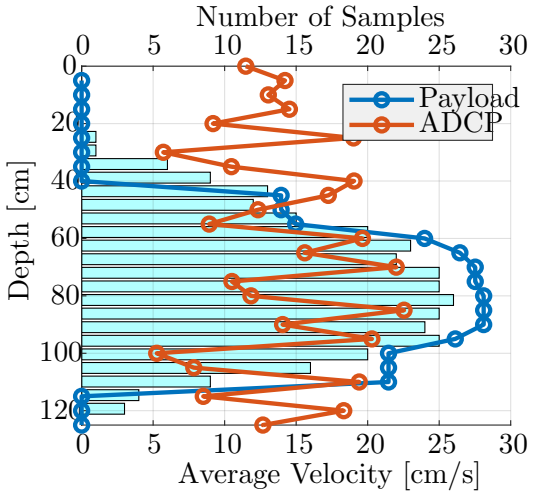

(c) Latitude 34.7810, Longitude -76.5740

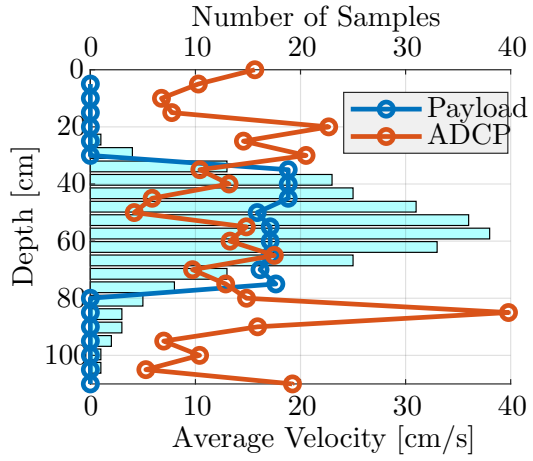

(d) Latitude 34.7809, Longitude -76.5739

Fig. A.2: March 14th, Velocity Profiles from Flights in Otway, NC. The ADCP failed to record velocities for profile (b).

CURRICULUM VITAE

Mitchell L. Bailey

Bachelor's Degree - Aerospace Engineering from Iowa State University, 2022.

Magna Cum Laude, Honors Program Graduate, Tau Beta Pi